14:53:50 OCA PAD INITIATION - PROJECT HEADER INFORMATION 01/28/92

Active

Project #: E-19-689 Cost share #: Rev #: 0
Center # : 10/24-6-R7394-0A0 Center shr #: OCA file #:
Work type : RES
Contract#: AGREEMENT DTD 1/13/92 Mod #: Document : AGR
Prime #: Contract entity: GTRC

Subprojects ? : N CFDA: N/A
Main project #: PE #: N/A

Project unit: CHEM ENGR Unit code: 02.010.114
Project director(s):
SCHORK F J CHEM ENGR (404)894-3274

Sponsor/division names: E I DUPONT DE NEMOURS CO /
Sponsor/division codes: 204 / 008

Award period: 920201 to 930131 (performance) 930131 (reports)

Sponsor amount	New this change	Total to date
Contract value	36,488.00	36,488.00
Funded	36,488.00	36,488.00
Cost sharing amount		0.00

Does subcontracting plan apply ?: N

Title: G-TYPE NEOPRENE LATEX AGING

PROJECT ADMINISTRATION DATA

OCA contact: Kathleen R. Ehlinger 894-4820

Sponsor technical contact

MR. BERTON BRODT
(504)536-5178

E.I. DUPONT DE NEMOURS AND COMPANY
P.O. BOX 2000
LAPLACE, LA 70068

Sponsor issuing office

MR. C.H. EVANS
(000)000-0000

E.I. DU PONT DE NEMOURS AND COMPANY
LEGAL DEPARTMENT - M-2618
1007 MARKET STREET
WILMINGTON, DE 19898

Security class (U,C,S,TS) : U ONR resident rep. is ACO (Y/N): N
Defense priority rating : N/A N/A supplemental sheet
Equipment title vests with: Sponsor GIT X
NONE PROPOSED.
Administrative comments -
INITIATION OF PROJECT. NOTE: THERE IS A PROPRIETARY AGREEMENT ON THIS PROJECT. SPONSOR INVOICED FOR ADVANCE PAYMENT OF $9,000.

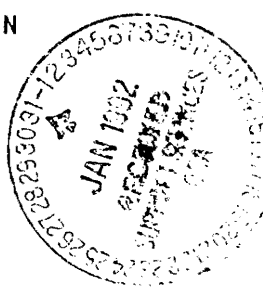

GEORGIA INSTITUTE OF TECHNOLOGY
OFFICE OF CONTRACT ADMINISTRATION

NOTICE OF PROJECT CLOSEOUT

Closeout Notice Date 08/05/93

Project No. E-19-689 Center No. 10/24-6-R7394-0A0

Project Director SCHORK F J School/Lab CHEM ENGR

Sponsor E I DUPONT DE NEMOURS CO/

Contract/Grant No. AGREEMENT DTD 1/13/92 Contract Entity GTRC

Prime Contract No.

Title G-TYPE NEOPRENE LATEX AGING

Effective Completion Date 930131 (Performance) 930131 (Reports)

Closeout Actions Required:	Y/N	Date Submitted
Final Invoice or Copy of Final Invoice	Y	930501
Final Report of Inventions and/or Subcontracts	N	
Government Property Inventory & Related Certificate	N	
Classified Material Certificate	N	
Release and Assignment	N	
Other	N	

CommentsEFFECTIVE DATE 2-1-92. CONTRACT VALUE $36,488.

Subproject Under Main Project No.

Continues Project No.

Distribution Required:

Project Director	Y
Administrative Network Representative	Y
GTRI Accounting/Grants and Contracts	Y
Procurement/Supply Services	Y
Research Property Managment	Y
Research Security Services	N
Reports Coordinator (OCA)	Y
GTRC	Y
Project File	Y
Other CARL BAXTER-FMD	Y
FRED CAIN-OOD	Y

MODELING THE ALKALINE AGING OF G-TYPE NEOPRENE LATEXES

A Report Prepared for E.I. du Pont de Nemours and Company Polymer Products Department

June 22, 1993

Work Done by: C.L. Liotta, F.J. Schork, C.M. Gilmore (author)
Schools of Chemistry and Chemical Engineering
Georgia Institute of Technology
Atlanta, GA 30332-0400,0100

ABSTRACT

G-Type Neoprene alkaline aging has been mathematically modeled based on a simplified mechanism involving simultaneous branching, scission and capping reactions. With key assumptions involving the unpeptized polymer MWD, molecular weight predictions, calculated from the leading moments of the polymer chain distributions, agree with experimental profiles and exhibit the expected sensitivity to peptizing agent concentrations. Residual peptizing agent and reactive site predictions are also consistent with analytical findings, but the observed particle size sensitivity is not fully explained by mass transfer effects.

TABLE OF CONTENTS

ABSTRACT 1
INTRODUCTION 3
SUMMARY AND CONCLUSIONS 3
RECOMMENDATIONS 5

DISCUSSION OF RESULTS 6

I. Process Description 6
A. Reactor Configuration 6
B. Reaction Mechanism and Kinetics 7
II. Mathematical Model Development 11
A. Mechanistic Assumptions 11
B. Fundamental Theories and Derivations 16
C. Mass Balances 17
D. Discrete Transformation, Moment Equations 21
E. Model Summary and Solution Requirements 23
III. Simulation Development 25
A. Computer Strategy 25
B. Parameter Estimation 25
IV. Simulation Results 29
A. Comparison with Laboratory Data 29
B. Sensitivity Analysis 38
C. Predictive Capability 45

REFERENCES 50

APPENDICES 51
I. Nomenclature 51
II. Neoprene Recipes, Experimental Results 52
III. Computer Program 55
A. Variable Notation 55
B. Program Listing 58
C. Sample Input/Output Files 66
IV. Indexing Terms 69

INTRODUCTION

The objective of this work, commissioned by DuPont to Georgia Tech [1], was to identify and mathematically model the mechanisms governing G-Type Neoprene alkaline aging, with the ultimate goal of facilitating quality improvement.

This report details progress made toward the accomplishment of this objective. The proposed mechanism[2] is restated, followed by the detailed mathematical model development, from the mass balances to the molecular weight moment equations. Finally, model validity is checked by comparison with laboratory data, and model sensitivity and predictive capability are assessed.

SUMMARY AND CONCLUSIONS

This report documents the progress of Georgia Tech personnel commissioned to 1) aid in the mechanistic understanding of G-Type Neoprene alkaline aging, and 2) produce a mathematical model of the associated peptization reactions.

In practice, G-Type Neoprene latex aging curves generally first exhibit a decrease, followed by a possible increase in Mooney viscosity, and are sensitive to latex particle size. Recent GPC data also suggest a sensitivity to the unpeptized polymer molecular weight distribution (MWD), as some peptization curves are characterized by an initial increase in molecular weight. While the details of this early increase are unresolved, mechanistically, the Mooney viscosity and molecular weight trends may be explained by a few key simultaneous scission, branching and capping reactions. Specifically, chain scission at the polysulfide sites is accomplished by the attack of dithiocarbamates (derived from tetraethylthiuram disulfide, TETD, or N,N-dibutyldithiocarbamate, Tepidone) on the sulfur-sulfur linkages of the copolymer. Branching results from the nucleophilic attack of a polymeric sulfide ion (derived from the scission reaction) on an allylic chloride or vinyl chloride group of another chain. Alternatively, the polymeric sulfide ion may be capped by reaction with TETD. The TETD/Tepidone ratio controls the capping/scission rate and thus determines molecular weight evolution. The mechanism is complicated by possible reversibility of the scission and capping reactions, and particle/aqueous-phase interfacial reactions.

The subject model (Model I) neglects these complications and also assumes that the unpeptized polymer is uniformly aged in a single well-mixed batch, is uniform with respect to reactive sites, and is characterized by a

unimodal MWD. The latex is assumed monodisperse, and the particle phase homogeneous. Tepidone uptake is modeled assuming a mass transfer resistance at the particle/aqueous-phase interface. Efforts aimed at relaxing some of these assumptions are reported separately (Models II,III).

Based on these assumptions, mass balances for the two polymer populations (uncharged and polymeric sulfide ions), reactive site, and peptizing agent concentrations were used to generate equations describing the three leading moments of each MWD. Model I then, comprised of 12 coupled ODEs, predicts the polymer weight and number-average molecular weights, and the Tepidone, TETD, and reactive site concentrations versus aging time. Major user-specified parameters, in addition to the recipe and other physical constants, include the latex and unpeptized polymer properties (*e.g.* MW_w, MW_n, D_p), rate constant Arrhenius parameters and medium correction factors, and Tepidone mass transfer parameters.

Model I predicted the laboratory peptization behavior of G-Type polymers that did not exhibit a large MW increase early in peptization (indicative of a persistent multimodal MWD with a preponderance of low MW chains). The MW_w and residual TETD profiles were in good agreement with measured values, and the predicted residual allylic chloride and S_6 site levels were qualitatively consistent with analytical findings.

Model I predictions of TETD and Tepidone effects were consistent with empirical observations and the proposed mechanism, *i.e.* the TETD/Tepidone ratio controlled the capping/scission rate and thus determined molecular weight evolution. Increasing the Tepidone level at a fixed, sufficient TETD concentration decreased MW_w, as did increasing the TETD level at a fixed Tepidone concentration.

Model I predictions of peptization rate were most sensitive to the scission rate constant and Tepidone level, while minimum MW_w predictions were sensitive to the capping and branching (allylic chloride only) rate constants. Increased/decreased sulfur incorporation was also observed to decrease/increase the final MW_w, while peptization rate predictions were also sensitive to the Tepidone partition coefficient, with an increase in affinity for the particle phase causing an increase in peptization rate. Order of magnitude changes in the Tepidone mass transfer coefficient also impacted peptization rate. However, with the monodispersed latex assumption, ±20% changes in the average particle diameter did not significantly affect Tepidone transfer.

RECOMMENDATIONS

- Model I use for general understanding of peptization variables.
- Model I use to aid development of peptization analytical techniques.
- Couple Model I with existing software to predict RTD effects.
- Continued model development to merge peptization chemistry and multimodal unpeptized polymer MWD.
- Analyze particle size effects with polydisperse latex.

DISCUSSION OF RESULTS

Mathematical modeling of a given process typically entails first, identification of the governing mechanisms, second, statement of the associated reaction kinetics, third, expression of the necessary mass and/or energy balances, fourth, application and/or development of appropriate mathematical solution techniques, and lastly, verification of the model predictions. This modeling strategy (Figure 1) was applied to the G-Type Neoprene alkaline aging process. Results are presently discussed.

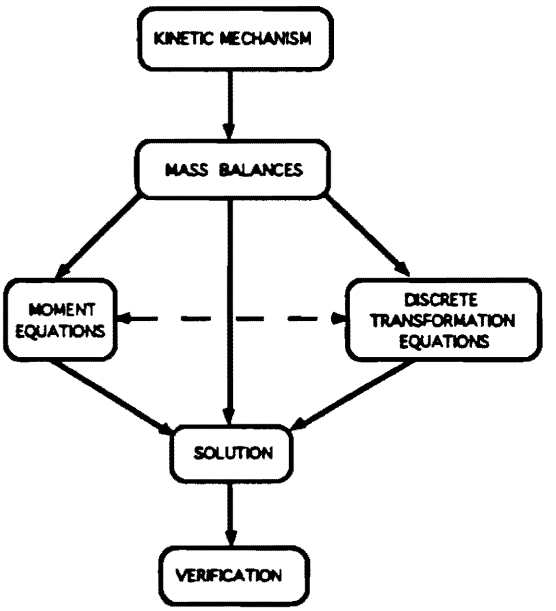

Figure 1: Modeling Schematic

I. Process Description

A. Reactor Configuration

In practice, G-Type Neoprenes may be aged over several vessels, and polymer exiting a given vessel is characterized by a residence time distribution. The subject model neglects these complications, and assumes the polymer is **uniformly aged in a single well-mixed batch.** Multiple vessel and non-ideal flow complications may be handled separately by solving the subject model in conjunction with suitable software.

B. Reaction Mechanism and Kinetics

Experimentally, G-Type Neoprene latex aging curves generally first exhibit a decrease, then an eventual increase in Mooney viscosity (Figure 2), and are sensitive to latex particle size. Note, however, that some experimental data[3] show an early increase in MW, followed by the expected MW decrease.[1] This data supports characterization of the peptization process by simultaneous MW-decreasing and MW-increasing reactions. As depicted in Figure 2, chain scission at the polysulfide sites is thought to dominate when the Mooney decreases, and branching and/or other MW-increasing reactions dominate when the viscosity increases. A proposed aging mechanism, accounting for simultaneous peptization/capping/branching and interphase mass transfer, has been reported[2], but is restated here (with some additions) for continuity.

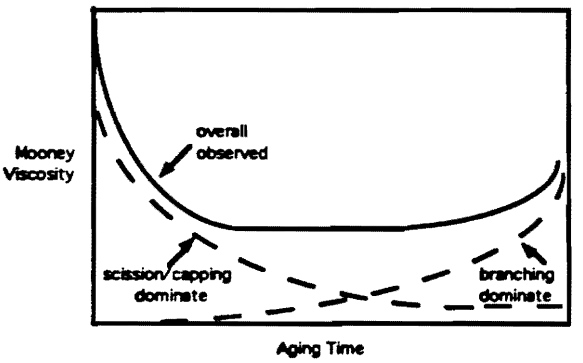

Figure 2: G-Type Neoprene Aging Curve (illustrative)

The reactions, listed in Table 1, represent three basic mechanisms: nucleophilic attack, acid-base equilibrium, and oxidation[2]. Nucleophilic attack is the dominant mechanism and may involve the attack of several nucleophiles (dithiocarbamate (T^-), hydroxide ion (OH^-), polymeric sulfide ion (S^-M_q)) on electrophilic disulfide bonds (chloroprene-sulfur copolymer (M_n), tetraethylthiuram disulfide (TETD, TT), mixed disulfide (T_bT_e)). Note that M_n is of arbitrary length and may be part of a branched network. Also, as depicted by the schematic in Figure 3, the reactions may occur in the particle phase and/or at the particle-aqueous phase interface, depending on the solubility of the involved species.

[1] As presented in Section IV.C., the author assumes a general positive correlation of Mooney viscosity with MW (Figure 23), realizing that Mooney viscosity actually depends on *parts* of the MWD *and* the peptization reactions occuring in the Mooney apparatus.

[2] Other unidentified reactions probably occur during peptization. Ongoing NMR studies suggest, at least, the formation of diethylamine[4].

Table 1: G-Type Neoprene Alkaline Aging — Proposed Mechanism[2]

#	Reaction	Type[a]	Site[b]	Other Comments
1	$M_n + T^- \xrightarrow{k_1} S^-M_q + M_{n-q}T$	NA	P,I	•Primary scission reaction •Occurs at any sulfur (except RS bond)
1a	$M_n + OH^- \xrightarrow{k_{1a}} S^-M_q + M_{n-q}OH$	NA	I	•OH^- *insoluble* in particle phase
2	$M_n + S^-M_q \xrightarrow{k_2} M_r + S^-M_m$	NA	P	•Molecular weight redistribution
3	$M_n + S^-M_q \xrightarrow{k_3} M_{n+q} + Cl^-$	NA	P	•Allylic chloride (cis 1,2 isomer) •Branching reaction
3a	$M_n + T^- \xrightarrow{k_3} M_n + Cl^-$			•Tepidone sink
4	$TT + OH^- \xrightarrow{k_4} T^- + TOH$	NA	I	•TT may be mixed disulfide
5	$T_eT_e + T_b^- \xrightarrow{k_5} T_bT_e + T_e^-$	NA	P,I	•Disulfide exchange •Occurs between any dithiocarbamate and any thiuram disulfide •Various sulfide ions kinetically indistinguishable
6	$TT + S^-M_q \xrightarrow{k_6} T^- + TSM_q$	NA	P	•Occurs with any thiuram disulfide
7	$M_n + S^-M_q \xrightarrow{k_7} M_{n+q} + Cl^-$	NA	P	•Vinyl chloride •Branching reaction •k_7 small, but $[VC]$ large
8	$RS^- + H_20 \rightleftharpoons RSH + OH^-$	ABE	I	• Hydrolysis of polymeric sulfide ion
9	$2RS^- + 2O_2 + 2H_20 \xrightarrow{k_9} RSSR + H_2O_2 + 2OH^-$	OXD	I	•Oxidation of polymeric sulfide ions •O_2 retards peptization

[a]Mechanism type: NA – nucleophilic attack, ABE – acid-base equil., OXD – oxidation

[b]Physical site of reaction: P – particle phase, I – particle interface

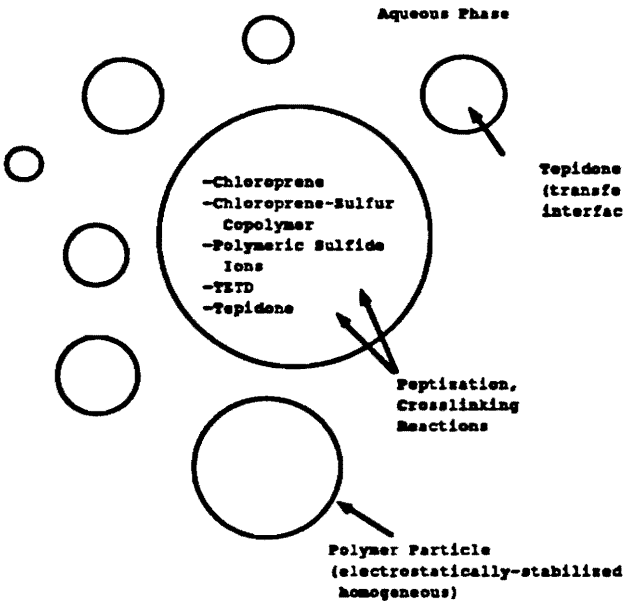

Figure 3: G-Type Neoprene Aging Mechanistic Schematic

The deceptively simple Table 1 reaction set actually encompasses complex equilibrium reactions and polymer structure/reactivity complications. Consider Reactions 1 and 2.

$$M_n + T^- \xrightarrow{k_1} M_{n-q}T + S^-M_q$$

$$M_n + S^-M_q \xrightarrow{k_2} M_r + S^-M_m$$

The capped chain from Reaction 1 ($M_{n-q}T$) may react with a polymeric sulfide ion (S^-M_q) according to Reaction 2. If the polymeric sulfide ion attacks the *terminal* sulfur linkage of the capped chain, a higher MW chain and a *pseudo* Tepidone are formed, *i.e.*

$$M_{n-q}T + S^-M_q \xrightarrow{k_2'} M_n + T^-$$

This is, in effect, the reverse of Reaction 1. Similarly, consider Reactions 6 and 1.

$$TT + S^-M_q \xrightarrow{k_6} M_qT + T^-$$

$$M_n + T^- \xrightarrow{k_1} M_{n-q}T + S^-M_q$$

The capped chain from Reaction 6 (M_qT) may react with Tepidone (T^-) according to Reaction 1. If Tepidone attacks the *terminal* sulfur linkage of the capped chain, a polymeric sulfide ion and a *pseudo* thiuram are formed, *i.e.*

$$M_qT + T^- \xrightarrow{k_1'} S^-M_q + TT$$

This is, in effect, the reverse of Reaction 6. Both Reaction 1 and Reaction 6 reverse reactions require chain scission at the *terminal* polysulfide site. The assumption that the ratio of *terminal* sites to intramolecular sites is small affords a potential modeling simplification.

The Table 1 reaction set is further complicated by the polymer structure and reactivity. Although conveniently characterized by an average molecular weight, the unpeptized polymer is obviously comprised of a distribution(s) of chain lengths, each potentially varying in intramolecular structure, *e.g.* allylic Cl sites, sulfur concentration and sequence length distribution. Thus, the polymer MWD may be uni- or multi-modal, and the reaction rate constants are functions of the number of sulfurs in the polysulfide linkage (sulfur rank).

Finally, in addition to the Table 1 reaction set, the proposed peptization mechanism accommodates dithiocarbamate (Tepidone, T^-) transfer from the aqueous phase into the particle:

$$(T^-)_{aq} \overset{k_m a}{\rightarrow} (T^-)_{particle}$$

The electrostatic double layer at the particle surface presents a resistance to transfer of the sulfide ion across the interface. According to this model, Tepidone uptake is governed by 1) the equilibrium partitioning of Tepidone between the particle and aqueous phases, 2) mass transfer resistance at the particle surface ($k_m a$), and 3) the rate of reaction of Tepidone inside the particle. Other, possibly less favorable, mechanisms are discussed in Reference [2].

II. Mathematical Model Development

A. Mechanistic Assumptions

As is evident from the proposed mechanism, the simplest of polymeric processes are often very complex, necessitating simplifying assumptions for successful modeling. The subject aging models incorporate several key assumptions (Table 2). The base assumptions apply to all models, while further simplifications are model-specific. Key assumptions requiring further elaboration are presently discussed. Minor assumptions (not listed in Table 2) are stated as appropriate in the subsequent text.

Table 2: Model Assumptions

	Model I	Model II	Model III
Base Assumptions			
Monodisperse latex	√	√	√
Homogeneous particle phase	√	√	√
Unpeptized polymer 100% soluble	√	√	√
Indistinguishable ion rxns negl.	√	√	√
Uniform allylic Cl	√	√	√
Chain scission arbitrary	√	√	√
Average rate constants	√	√	√
Other Simplifications			
Interfacial rxns negl.	√		√
Unimodal MWD	√	√	
Uniform sulfur dist.	√	√	
Scission at *end* site negl.	√		√
Reactions 1',2' negl.	√		√
Capped/Uncapped negl. (*i.e.* $M_nT{=}M_n$)	√		√
Tepidone sink (allylic Cl) negl.	√		√

Base Assumptions (all models)

The unpeptized polymer is present in latex particles which are assumed spherical and of uniform diameter and compostion. Relaxing the monodisperse PSD assumption does not significantly complicate modeling equations, but computation time is increased since the equations are solved repeatedly for several particle sizes. On the other hand, the homogeneous particle phase assumption avoids the complexity of partial differential equations since any radial dependence of species concentrations is neglected. This assumption is potentially significant since several reactions involve partially water-soluble species.

The unpeptized polymer is further assumed to be 100% soluble[3]. This is in contrast to earlier thought that a fraction of the polymer was insoluble, presumably due to crosslinking and/or excessive entanglement. A given polymer chain is assumed uniform with respect to intramolecular branching sites (*e.g.* allylic Cl) and polysulfide linkages. Allylic Cl may be relatively evenly distributed, but sulfur is probably not uniformly incorporated during polymerization[5]. Nonetheless, with the assumption of uniform intramolecular sulfur distribution, scission may occur arbitrarily at any site along the chain. The polysulfide linkages may contain 2 to 8 sulfurs, but the S_6 configuration appears prevalent[6], and is therefore assumed exclusively. Accordingly, average rate constants are used, but compensation is made for a general reduction in rate constants with decreased sulfur rank.

Other Assumptions (model-specific)

While all of the subject models incorporate the base assumptions, they may be distinguished based on characterization of the unpeptized polymer MWD and treatment of certain end-chain and interfacial reactions. Specifically, both Models I and II assume that the unpeptized polymer MWD is unimodal, but GPC results[3] show a definite multimodality (Figures 4 and 5), which may (Figure 5) or may not (Figure 4) persist after the onset of peptization. More importantly, peptization appears very sensitive to the unpeptized polymer structure. Thus, Model III assumes a trimodal MWD, and also accommodates an overall variance of sulfur incorporation with polymer molecular weight, *i.e.* polymer in a given MW fraction may contain more or less sulfur than that in another fraction. This affords a possible means of adjusting relative reactivities without altering rate constants.

Like Model I, however, Model III neglects interfacial reactions (1a,4,8, and 9 in Table 1) and reactions decribing scission at the terminal sulfur linkage of a capped chain. First, consider the interfacial reaction assumption. Doyle[7] measured a definite, but slow reduction in Mooney viscosity after adding TETD only to a G-Type Neoprene. This may be explained by the reaction of

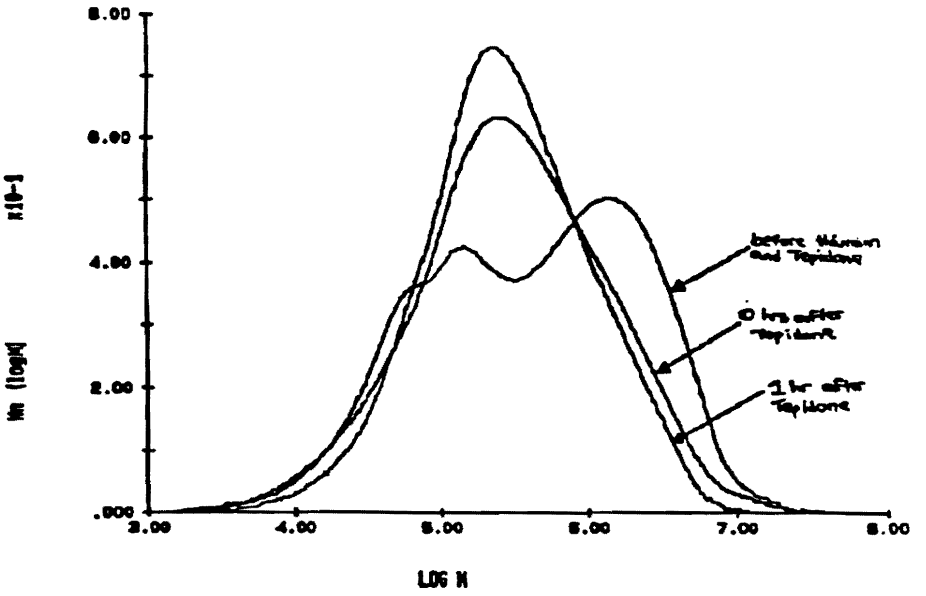

Figure 4: MWD(GPC) vs Aging Time for Run 4[3].

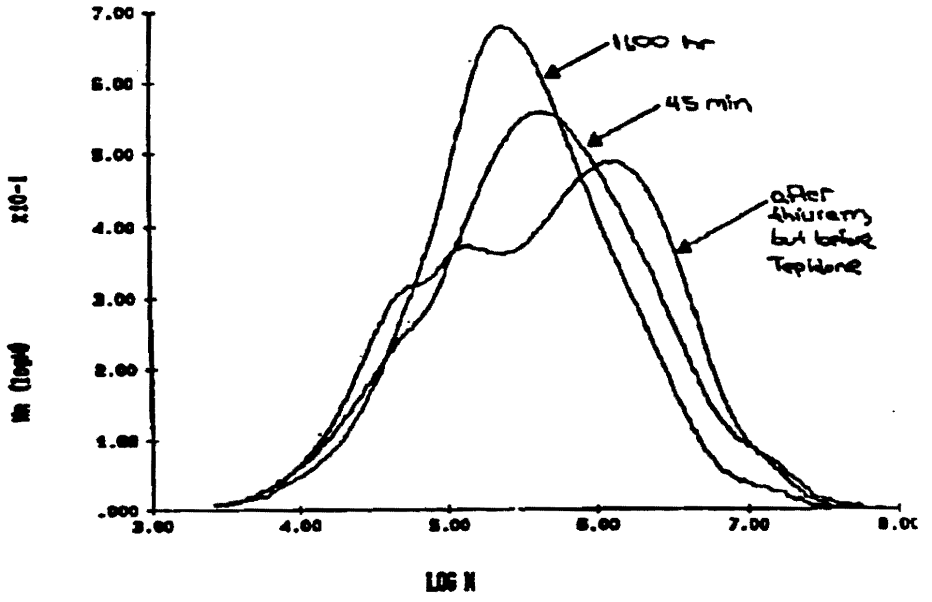

Figure 5: MWD(GPC) vs Aging Time for Run 2[3].

TETD with OH^- to yield T^- (Reaction 4), and subsequent chain scission via Reaction 1. The observed slow Mooney reduction (compared to that observed with both TETD and Tepidone added) suggests that Reaction 4, and thus Reaction 1a, may be neglected. Recent GPC measurements[3], however, show a significant change in MW after TETD, but before Tepidone addition (Table 3), suggesting the significance of interfacial and/or unidentified reactions. Model II includes Reactions 1a and 4, but assumes a constant low $[OH^-]$. Alternatively, Reaction 4 effects may be estimated by assuming a fraction of the added TETD is *lost* to T^-, perhaps during the quick transfer to the particle phase.

Table 3: Average MW for Unpeptized and Thiuram Only Samples[3].

		Unpeptized	With TETD Only
Run 2	MW_n	108,000	105,000
	MW_w	854,000	1,408,000
Run 6	MW_n	105,000	114,000
	MW_w	1,579,000	625,000

Next consider the reactions describing scission at the terminal sulfur linkage of a capped chain. Specifically,

$$M_nT + T^- \xrightarrow{k_1'} S^-M_n + TT$$

$$M_{n-q}T + S^-M_q \xrightarrow{k_2'} M_n + T^-$$

NMR analysis of model compound reactions with Tepidone only[4,6] and separate analysis of Tepidone uptake data[6] with no TETD added revealed no TETD formation. This suggests that k_6 is much larger than k_1', a conclusion also supported by kinetic studies[6]. On the other hand, kinetic studies estimated k_2' at roughly an order of magnitude greater than k_1 and NMR analysis indicated little capped product in the absence of TETD, both potentially supporting the relative significance of Reaction 2'. NMR results also indicate, however, that the capped product is unstable, somehow decomposing to a polymeric sulfide ion and diethylamine. This suggests that the unidentified decomposition rate constant is larger than k_2', thus explaining the absence of capped product when only Tepidone is added. More pertinent to MW considerations, Reaction 2' may not afford a net MW increase since it would follow Reaction 1 and it is unlikely that a higher MW capped chain or polymeric sulfide ion would preempt the Reaction 1 products. Reaction with a capped product from Reaction 6 would result in a higher MW species, but further chain scission is probable (Reaction 2' also generates a Tepidone) since TETD *sustains* reduced MW. The net effect of Reaction 2 could be a

higher equilibrium particle-phase Tepidone concentration. Lastly, note that Reaction 2 may effect a MW increase via scission *near* the chain end, *e.g.*

	$M_5 + S_{15}^- \xrightarrow{k_2}$	$M_2 + S_{18}^-$
M_n	10	10
M_w	12.5	16.4

Neglecting the end-chain reactions eliminates the need for tracking the capped species and reduces the number of model equations. Models I and III incorporate this simplification, while Model II includes the end-chain reactions.

Finally, consider Tepidone reaction at the allylic Cl (Reaction 3a). While kinetic measurements[6] support inclusion of this reaction as a true Tepidone sink, Tepidone uptake measurements (Figure 6) do not show a significant continual decrease in the aqueous phase Tepidone concentration when allylic Cl is undoubtedly present[3]. Reaction 3a is omitted from Models I and III, but is included in Model II.

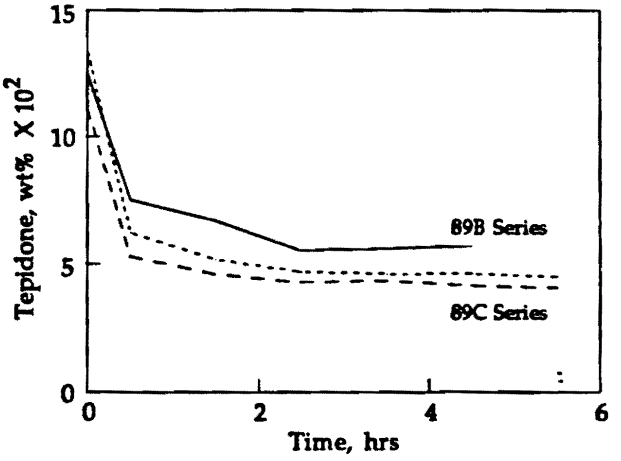

Figure 6: Tepidone Uptake with Neoprene GRT Latex at 40°C[6].

Many of the model-specific assumptions resulted from mechanistic insight gained and/or emphasized after modeling efforts were well underway. **Thus, the first model, Model I, has been analyzed most completely, and is emphasized in subsequent discussion.**

B. Fundamental Theories and Derivations

Having proposed the mechanism governing the aging process, and identified key simplifying assumptions, construction of the model equations follows. Here, the fundamental principles of mass balances, discrete transformation, and moment representations are employed. A brief discussion of these principles follows. The reader is referred to References [8]–[10] for more detail.

For this batch system, mass balances are of the form

$$\left\{\begin{array}{c}\text{change}\\ \text{in concentration}\\ \text{with time}\end{array}\right\} = \left\{\begin{array}{c}\text{total rate of addition}\\ \text{or depletion of concentration}\\ \text{by various mechanisms}\end{array}\right\} \tag{1}$$

and may be written for the polymer chain populations (M_n and $S^- M_n$), along with other species, to obtain a complete differential molecular weight distribution (MWD).

The mass balances constitute an infinite set (n from 1 to ∞) of coupled ordinary differential equations (ODEs). Aside from the obvious calculational difficulties, the routine use of full differential MWDs to represent the state of reacting polymer is often impractical or impossible. It is more convenient to use the leading moments of the differential MWD. For the populations M_n and S_n, the kth moments are defined as

$$\begin{aligned}\eta_k &= \sum_{n=1}^{\infty} n^k M_n \quad k = 0,1,2,...\\ \lambda_k &= \sum_{n=1}^{\infty} n^k S_n \quad k = 0,1,2,...\end{aligned} \tag{2}$$

and the number and weight-average molecular weights (MW_n, MW_w) as

$$MW_n = w\left[x_M\left(\frac{\eta_1}{\eta_0}\right) + x_S\left(\frac{\lambda_1}{\lambda_0}\right)\right] \tag{3}$$

$$MW_w = w\left[x_M\left(\frac{\eta_2}{\eta_1}\right) + x_S\left(\frac{\lambda_2}{\lambda_1}\right)\right] \tag{4}$$

$$PD = MW_w/MW_n \tag{5}$$

where w is the mer molecular weight and x_M and x_S are the weight fractions of the M_n and S_n populations, respectively. PD is the polydispersity.

Obviously, the moment equations may be obtained directly from Eqn. (2) by the indicated series summation of the mass balances, i.e.

$$\frac{d\eta_k}{dt} = \sum_{n=1}^{\infty} n^k \frac{dM_n}{dt} \tag{6}$$

but it is generally easier to use a discrete transformation technique, such as Z-transforms, and then extract the moments. Given the population M_n, the Z-transform is defined as

$$\mathcal{M}(z) = \sum_{n=0}^{\infty} M_n z^{-n} \tag{7}$$

and the infinite set of ODEs is transformed to a single equation for $\frac{d\mathcal{M}(z)}{dt}$. The moment equations become

$$\eta_k = \left[(-1)^k \frac{\partial^k \mathcal{M}(z)}{\partial (lnz)^k}\right]_{z \to 1} \tag{8}$$

or

$$\frac{d\eta_k}{dt} = \frac{d}{dt}\left[(-1)^k \frac{\partial^k \mathcal{M}(z)}{\partial (lnz)^k}\right]_{z \to 1} \tag{9}$$

and a set of three moment equations ($\frac{d\eta_0}{dt}$, $\frac{d\eta_1}{dt}$, $\frac{d\eta_2}{dt}$) replaces the $\frac{d\mathcal{M}(z)}{dt}$ equation.

As is the case in many polymer systems, here, the equation for η_2 depends on η_3. As pointed out by Tirrell[10], this generally occurs when a polymer participates in a reaction which can occur at *every* monomer unit along the chain, and not only at the ends. This is the case in Reactions 1 and 2, where the nucleophile (T^- or S^-M_q) may attack the polymer chain (M_n) at any monomer unit. Tirrell further applies a moment closure procedure using the associated Laguerre polynomials to obtain the following expression for an arbitrary distribution described as a perturbation around a T-distribution:

$$\eta_3 = \frac{\eta_2}{\eta_0 \eta_1}(2\eta_0\eta_2 - \eta_1^2) \tag{10}$$

With this substitution[3], the set of moment equations may be solved numerically.

C. Mass Balances

Using the form of Eqn. (1), Model I mass balances are written for the polymer populations (M_n and S^-M_n), the polysulfide (RS), allylic chloride (AC), and vinyl chloride (VC) reactive sites, and the Tepidone (aqueous T_w, particle T_p) and TETD (TT) concentrations. Balances are based on the simplified mechanism listed in Table 4.

[3]Substitution of the moment expressions for M_n, M_w, and M_z into Eqn. (10) yields $M_z = 2M_w - M_n$, an obvious underestimation.

Table 4: G-Type Neoprene Alkaline Aging — Model I Mechanism[2]

#	Reaction
1	$M_n + T^- \xrightarrow{k_1} S^-M_q + M_{n-q}T$
2	$M_n + S^-M_q \xrightarrow{k_2} M_r + S^-M_m$
3	$M_n + S^-M_q \xrightarrow{k_3} M_{n+q} + Cl^-$
6	$TT + S^-M_q \xrightarrow{k_6} T^- + TSM_q$
7	$M_n + S^-M_q \xrightarrow{k_7} M_{n+q} + Cl^-$

Uncharged Polymer Population, M_n

Noting that M_n, M_nT, and TSM_n are equivalent, and S^-M_n may be written as S_n for simplicity, the mass balance on species M_n ($n = 1, 2, \ldots$; $M_0 = S_0 = 0$) is given by

$$\begin{aligned}\frac{dM_n}{dt} &= k_1T_pf_s\sum_{q=n+1}^{\infty}M_q - k_1T_pf_s(n-1)M_n \\ &+k_2f_s\sum_{q=0}^{n-1}S_q\sum_{p=(n-q)+1}^{\infty}M_p - k_2f_s(n-1)M_n\sum_{q=1}^{\infty}S_q \\ &+k_3f_a\sum_{q=1}^{n-1}qM_qS_{n-q} - k_3f_anM_n\sum_{q=1}^{\infty}S_q \\ &+k_7f_v\sum_{q=1}^{n-1}qM_qS_{n-q} - k_7f_vnM_n\sum_{q=1}^{\infty}S_q + k_6[TT]S_n \end{aligned} \quad (11)$$

where f_s, f_a and f_v are the fraction of polysulfide linkages, allylic chlorides, and vinyl chlorides in the polymer chain (moles reactive sites/mole mer). The equation form reflects the rate dependence on the *number of reactive sites*, not the polymer concentration.

Polymeric Sulfide Ions, S^-M_n or S_n

The mass balance on species S_n is given by

$$\begin{aligned}\frac{dS_n}{dt} &= k_1T_pf_s\sum_{q=n+1}^{\infty}M_q + k_2f_s\sum_{q=1}^{\infty}S_q\sum_{p=n}^{\infty}M_p \\ &+k_2f_sS_n\sum_{p=1}^{\infty}pM_p - k_3f_aS_n\sum_{q=1}^{\infty}qM_q \\ &-k_7f_vS_n\sum_{q=1}^{\infty}qM_q - k_6[TT]S_n \end{aligned} \quad (12)$$

Polysulfide Reactive Sites, $[RS]$

The mass balance on the polysulfide reactive sites is potentially complicated by the fact that each linkage of 3 or more sulfurs provides more than one reactive site. Thus, the effect of each of the reactions on $[RS]$ depends upon the length of the sulfur linkages in M_n and S_q, and/or where the scission occurs. For example, as indicated below, for a given scission, Reaction 2 could increase, decrease, or not affect $[RS]$.

$$\begin{aligned} R_1 - S_4^- + R_2 - S_6 - R_3 & \qquad \text{(5 sites)} \\ \xrightarrow{k_2} R_1 - S_8 - R_2 + R_3 - S_2^- & \qquad \text{(7 sites)} \\ \xrightarrow{k_2} R_1 - S_5 - R_2 + R_3 - S_5^- & \qquad \text{(4 sites)} \\ \xrightarrow{k_2} R_1 - S_6 - R_2 + R_3 - S_4^- & \qquad \text{(5 sites)} \end{aligned}$$

In the above example, the composition of R_1, R_2 and R_3 also affect $[RS]$. To avoid this complexity, the balance is written for the polysulfide linkage concentration, effectively assuming each linkage provides one reactive site. Thus,

$$\begin{aligned} \frac{d[RS]}{dt} &= -k_1 T_p f_s \sum_{n=1}^{\infty}(n-1)M_n + k_3 f_a S_n \sum_{q=1}^{\infty} qM_q \\ &\quad + k_6[TT]\lambda_0 + k_7 f_v S_n \sum_{q=1}^{\infty} qM_q \end{aligned} \tag{13}$$

To convert $[RS]$ (mole sites/cc-part) to f_s (mole sites/ moles mer), divide by the total mer concentration, i.e.

$$f_s = \frac{[RS]}{\eta_1 + \lambda_1} \tag{14}$$

Eqn. (15) affords a virtual *conservation* of reactive sites and necessitates an independent reduction of rate constants with sulfur rank reduction. Alternatively, one might track the depletion of S_6 linkages via Reaction 1 only, and assume each S_6 scission yields two less reactive S_2, S_3, or S_4 linkages. A reduced rate constant ($k_{1,red} = k_1 \cdot$ *reduction factor*) would then apply to the low sulfur rank sites, and $k_1 f_s$ would be expanded to $[k_1 f_s + 2k_{1,red}(f_{so} - f_s)]$ in the other rate expressions. The Model I code reflects this alternate approach; for brevity, $k_1 f_s$ is not expanded in the text. A similar treatment is applied to $k_2 f_s$.

Allylic Chloride Sites, $[AC]$

Allylic chloride sites in the soluble fraction are expressed by

$$\frac{d[AC]}{dt} = -k_3 f_a S_n \sum_{q=1}^{\infty} qM_q \tag{15}$$

where

$$f_a = \frac{[AC]}{\eta_1 + \lambda_1} \tag{16}$$

Vinyl Chloride Sites, $[VC]$

Vinyl chloride sites in the soluble fraction are expressed by

$$\frac{d[VC]}{dt} = -k_7 f_v S_n \sum_{q=1}^{\infty} q M_q \tag{17}$$

where

$$f_v = \frac{[VC]}{\eta_1 + \lambda_1} \tag{18}$$

Tepidone, T_w and T_p

By assumption, the Tepidone is initially present in the aqueous phase (T_w), and then transfers to the particle (T_p), the driving force being the departure from equilibrium concentrations. T_w is given by

$$\frac{dT_w}{dt} = -\frac{k_m A_p}{V_w}\left[T_w - \left(\frac{1}{PC}\right)T_p\right] \tag{19}$$

where PC is the partition coefficient, i.e. $(T_p/T_w)_{equil}$. Similarly, Tepidone enters the particles at the same rate, is consumed by Reaction 1, and produced by Reaction 6. Thus,

$$\begin{aligned}\frac{dT_p}{dt} &= \frac{k_m a_p}{v_p}\left[T_w - \left(\frac{1}{PC}\right)T_p\right] - k_1 T_p f_s \sum_{n=1}^{\infty}(n-1)M_n \\ &\quad + k_6[TT]\sum_{n=1}^{\infty} S_n\end{aligned} \tag{20}$$

Tetraethylthiuram Disulfide, $[TT]$

By assumption, TETD is exclusively in the particle phase at the beginning of peptization. It is consumed by Reaction 6. Thus,

$$\frac{d[TT]}{dt} = -k_6[TT]\sum_{n=1}^{\infty} S_n \tag{21}$$

Table 5: Z-Transforms

Function	Z-Transform
M_n	$\mathcal{M}(z) = \sum_{n=0}^{\infty} M_n z^{-n}$
c	$c\left(\frac{z}{z-1}\right)$
$\sum_{q=1}^{n} M_q$	$\mathcal{M}(z)\left(\frac{z}{z-1}\right)$
nM_n	$-z\frac{\partial \mathcal{M}(z)}{\partial z}$
$\sum_{q=1}^{n-1} qM_q S_{(n-q)}$	$-\mathcal{S}(z)\frac{\partial \mathcal{M}(z)}{\partial z}$

D. Discrete Transformation, Moment Equations

As outlined in Section II.B., the infinite set of mass balances is transformed to a finite, solvable set by employing Z-transforms, and the associated moment generation property. Using the Z-transforms in Table 5 and the moment definitions in Eqn. (2), each term in Eqns. (13) and (14) is transformed to yield

$$\begin{aligned}
\frac{d\mathcal{M}(z)}{dt} &= k_1 T_p f_s \left(\frac{\eta_0 - z\mathcal{M}(z)}{z-1}\right) - k_1 T_p f_s \left[\sum_{n-1}^{\infty} nz^{-n} M_n - \mathcal{M}(z)\right] \\
&+ \mathcal{Z}\left(k_2 f_s \sum_{q=0}^{n-1} S_q \sum_{p=(n-q)+1}^{\infty} M_p\right) - k_2 f_s \lambda_0 \left[\sum_{n-1}^{\infty} nz^{-n} M_n - \mathcal{M}(z)\right] \\
&+ k_3 f_a \mathcal{S}(z)\left(\sum_{n=1}^{\infty} nz^{-(n+1)} M_n\right) - k_3 f_a \lambda_0 \sum_{n=1}^{\infty} nz^{-n} M_n \\
&+ k_7 f_v \mathcal{S}(z)\left(\sum_{n=1}^{\infty} nz^{-(n+1)} M_n\right) - k_7 f_v \lambda_0 \sum_{n=1}^{\infty} nz^{-n} M_n \\
&+ k_6 [TT]\mathcal{S}(z) \qquad (22)
\end{aligned}$$

and

$$\frac{dS(z)}{dt} = k_1 T_p f_s \left(\frac{\eta_0 - z\mathcal{M}(z)}{z-1}\right) + k_2 f_s \lambda_0 \left(\frac{\eta_0 - z\mathcal{M}(z)}{z-1}\right) - k_6[TT]S(z)$$
$$-k_2 f_s(\eta_1 - \eta_0)S(z) - k_3 f_a \eta_1 S(z) - k_7 f_v \eta_1 S(z) \quad (23)$$

The Z-transform of the third term in Eqn. (11) is not easily identified, so the contribution to the moment equations is calculated directly from the mass balance (Eqn. (6)). For the remaining terms, the moment contributions are calculated by evaluating Eqn. (9). Specifically, for Eqn. (22),

$$\frac{d\eta_0}{dt} = \frac{d\mathcal{M}(z)}{dt}|_{z\to 1}$$
$$\frac{d\eta_1}{dt} = \frac{d}{dt}\left(-z\frac{\partial \mathcal{M}(z)}{\partial z}|_{z\to 1}\right)$$
$$\frac{d\eta_2}{dt} = \frac{d}{dt}\left(z\frac{\partial}{\partial z}\left(z\frac{\partial \mathcal{M}(z)}{\partial z}\right)\right)|_{z\to 1}$$

Similar equations apply for the S_n distribution ($\lambda_{0,1,2}$). The differentiation becomes tedious, as the limit evaluation requires repeated use of L'Hopital's Rule, and is greatly facilitated by the use of a math software package, e.g. *Mathematica*. After simplifying, the moment equations are given by

$$\frac{d\eta_0}{dt} = k_6[TT]\lambda_0 \quad (24)$$

$$\frac{d\eta_1}{dt} = -\frac{k_1 T_p f_s}{2}(\eta_2 - \eta_1) + k_2 f_s\left[\lambda_1(\eta_1 - \eta_0) - \frac{\lambda_0}{2}(\eta_2 - \eta_1)\right]$$
$$+k_3 f_a \lambda_1 \eta_1 + k_6[TT]\lambda_1 + k_7 f_v \lambda_1 \eta_1 \quad (25)$$

$$\frac{d\eta_2}{dt} = \frac{k_1 T_p f_s}{6}(\eta_1 + 3\eta_2 - 4\eta_3) + k_3 f_a(2\lambda_1\eta_2 + \lambda_2\eta_1)$$
$$+k_2 f_s\left[\lambda_2(\eta_1 - \eta_0) + \lambda_1(\eta_2 - \eta_1) - \frac{\lambda_0}{6}(4\eta_3 - 3\eta_2 + \eta_1)\right]$$
$$+k_6[TT]\lambda_2 + k_7 f_v(2\lambda_1\eta_2 + \lambda_2\eta_1) \quad (26)$$

$$\frac{d\lambda_0}{dt} = k_1 T_p f_s(\eta_1 - \eta_0) - k_3 f_a \eta_1 \lambda_0 - k_6[TT]\lambda_0 - k_7 f_v \eta_1 \lambda_0 \quad (27)$$

$$\frac{d\lambda_1}{dt} = \frac{k_1 T_p f_s}{2}(\eta_2 - \eta_1) - k_2 f_s\left[\lambda_1(\eta_1 - \eta_0) - \frac{\lambda_0}{2}(\eta_2 - \eta_1)\right]$$
$$-k_3 f_a \lambda_1 \eta_1 - k_6[TT]\lambda_1 - k_7 f_v \lambda_1 \eta_1 \quad (28)$$

$$\frac{d\lambda_2}{dt} = \frac{k_1 T_p f_s}{6}(2\eta_3 - 3\eta_2 + \eta_1) + \frac{k_2 f_s \lambda_0}{6}(2\eta_3 - 3\eta_2 + \eta_1)$$
$$-k_2 f_s \lambda_2(\eta_1 - \eta_0) - k_3 f_a \eta_1 \lambda_2 - k_6[TT]\lambda_2 - k_7 f_v \eta_1 \lambda_2 \quad (29)$$

Given the extent of mathematical manipulation required to obtain the moment equations, a cursory check of the equations against the simplified mechanism (Table 4) is appropriate. First, the total number of mers is constant, i.e.

$$\frac{d\eta_1}{dt} + \frac{d\lambda_1}{dt} = 0$$

Second, η_0, the total concentration of M_n chains, is increased by Reaction 6 only while λ_0, the total concentration of S_n chains, is increased by Reaction 1, and decreased by Reactions 3, 6, and 7.

Lastly, consider the molecular weight effects predicted by the moment equations (Table 6). The effects were predicted by isolating the moment contributions from each reaction and applying the molecular weight definitions in Eqns. (3) and (4). As expected, Reaction 1 can only decrease MW, Reactions 3 and 7 can only increase MW, and Reaction 6 has no direct effect. Reaction 2, however, has no effect on MW_n, but can either increase or decrease MW_w since

$$\left(\frac{d\eta_2}{dt} + \frac{d\lambda_2}{dt}\right)_{Rxn2} = k_2 f_s \left[\lambda_1(\eta_2 - \eta_1) + \frac{\lambda_0}{3}(\eta_1 - \eta_3)\right]$$

Consideration of these effects is useful when tuning model parameters.

Table 6: Predicted Qualitative MW Effects

	Effect on ...	
Rxn	MW_w	MW_n
1	↓	↓
2	↑↓	-
3,7	↑	↑
6	-	-

E. Model Summary and Solution Requirements

In summary, based on the simplified mechanism of Table 4, Model I predicts the polymer number and weight-average molecular weights, and the Tepidone, TETD, and reactive site concentrations versus aging time. It is comprised of the following 12, coupled ODEs[4]:

$$\frac{dT_w}{dt} = -\frac{k_m A_p}{V_w}\left[T_w - \left(\frac{1}{PC}\right)T_p\right] \tag{30}$$

[4]In application, only the first RHS term in Eqn (39) is retained and $k_1 f_s$ is expanded to $[k_1 f_s + 2k_{1,red}(f_{so}\text{-}f_s)]$ in other rate expressions. A similar treatment is applied to $k_2 f_s$.

$$\frac{dT_p}{dt} = \frac{k_m a_p}{v_p}\left[T_w - \left(\frac{1}{PC}\right)T_p\right] - k_1 T_p f_s(\eta_1 - \eta_0) + k_6[TT]\lambda_0 \quad (31)$$

$$\frac{d[TT]}{dt} = -k_6[TT]\lambda_0 \quad (32)$$

$$\frac{d\eta_0}{dt} = k_6[TT]\lambda_0 \quad (33)$$

$$\frac{d\eta_1}{dt} = -\frac{k_1 T_p f_s}{2}(\eta_2 - \eta_1) + k_2 f_s\left[\lambda_1(\eta_1 - \eta_0) - \frac{\lambda_0}{2}(\eta_2 - \eta_1)\right] + k_3 f_a \lambda_1 \eta_1 + k_6[TT]\lambda_1 + k_7 f_v \lambda_1 \eta_1 \quad (34)$$

$$\frac{d\eta_2}{dt} = \frac{k_1 T_p f_s}{6}(\eta_1 + 3\eta_2 - 4\eta_3) + k_3 f_a(2\lambda_1\eta_2 + \lambda_2\eta_1) + k_2 f_s\left[\lambda_2(\eta_1 - \eta_0) + \lambda_1(\eta_2 - \eta_1) - \frac{\lambda_0}{6}(4\eta_3 - 3\eta_2 + \eta_1)\right] + k_6[TT]\lambda_2 + k_7 f_v(2\lambda_1\eta_2 + \lambda_2\eta_1) \quad (35)$$

$$\frac{d\lambda_0}{dt} = k_1 T_p f_s(\eta_1 - \eta_0) - k_3 f_a \eta_1 \lambda_0 - k_6[TT]\lambda_0 - k_7 f_v \eta_1 \lambda_0 \quad (36)$$

$$\frac{d\lambda_1}{dt} = \frac{k_1 T_p f_s}{2}(\eta_2 - \eta_1) - k_2 f_s\left[\lambda_1(\eta_1 - \eta_0) - \frac{\lambda_0}{2}(\eta_2 - \eta_1)\right] - k_3 f_a \lambda_1 \eta_1 - k_6[TT]\lambda_1 - k_7 f_v \lambda_1 \eta_1 \quad (37)$$

$$\frac{d\lambda_2}{dt} = \frac{k_1 T_p f_s}{6}(2\eta_3 - 3\eta_2 + \eta_1) + \frac{k_2 f_s \lambda_0}{6}(2\eta_3 - 3\eta_2 + \eta_1) - k_2 f_s \lambda_2(\eta_1 - \eta_0) - k_3 f_a \eta_1 \lambda_2 - k_6[TT]\lambda_2 - k_7 f_v \eta_1 \lambda_2 \quad (38)$$

$$\frac{d[RS]}{dt} = -k_1 T_p f_s(\eta_1 - \eta_0) + (k_3 f_a + k_7 f_v)\eta_1 \lambda_0 + k_6[TT]\lambda_0 \quad (39)$$

$$\frac{d[AC]}{dt} = -k_3 f_a \eta_1 \lambda_0 \quad (40)$$

$$\frac{d[VC]}{dt} = -k_7 f_v \eta_1 \lambda_0 \quad (41)$$

Supporting algebraic expressions include:

$$\eta_3 = \frac{\eta_2}{\eta_0 \eta_1}(2\eta_0\eta_2 - \eta_1^2)$$

$$f_s = \frac{[RS]}{\eta_1 + \lambda_1}$$

$$f_a = \frac{[AC]}{\eta_1 + \lambda_1}$$

$$f_v = \frac{[VC]}{\eta_1 + \lambda_1}$$

$$MW_n = w\left[x_M\left(\frac{\eta_1}{\eta_0}\right) + x_S\left(\frac{\lambda_1}{\lambda_0}\right)\right]$$

$$MW_w = w\left[x_M\left(\frac{\eta_2}{\eta_1}\right) + x_S\left(\frac{\lambda_2}{\lambda_1}\right)\right]$$
$$PD = MW_w/MW_n$$

where w is the mer molecular weight and x_M and x_S are the weight fractions of the M_n and S_n populations, respectively. Simple algebraic equations, detailed in Appendix III, are also used to calculate initial conditions from user-supplied data. Specifically, the user specifies the unpeptized polymer MWD, the weight-average particle diameter, recipe variables, reaction rate constant parameters, and other physical constants. Sample data files are also included in Appendix III.

III. Simulation Development

A. Computer Strategy

The FORTRAN code used to solve Model I is charted in Figure 7 and detailed in Appendix III. The subroutine ALGBR reads the input data files (RCP1 and CNST1) and calculates the initial conditions for the ODEs, which are numerically integrated using Gear's backward differentiation method. The IVPAG subroutine is available as part of the International Mathematical and Statistical Library (IMSL) software package. Results are written to three output files, MOLWGT, SITES, and MOMENT, examples of which are also included in Appendix III. The FORTRAN code is executed on a Digital Equipment Corporation VAX 6210.

B. Parameter Estimation

Most of the crucial model parameters were unavailable in the literature, and estimates were obtained from a kinetic study by S. Arthur[6]. The reader is referred to Reference [6] for experimental details and discussion, but rate constant estimates are presented in Table 7.

Assuming an Arrhenius dependence is applicable, i.e.

$$k = Aexp\left(-\frac{E}{RT}\right)$$

a plot of $\ln k$ vs. $\frac{1}{T}$ is characterized by a slope of $-\frac{E}{R}$ and an intercept equal to $\ln A$. Table 8 lists the calculated Arrhenius parameters, assuming k_1 and k_6 have the same temperature dependence, as do k_2 and k_3 (by assumption). In the absence of explicit data, these assumptions are made since Reactions 1 and 6 involve similar molecules, as do Reactions 2 and 3.

The rate constants reported in Table 7 were measured in both an 85:15 acetonitrile/water solution and methylene chloride, the polarity of which is thought to more closely resemble that of the particle. While potential

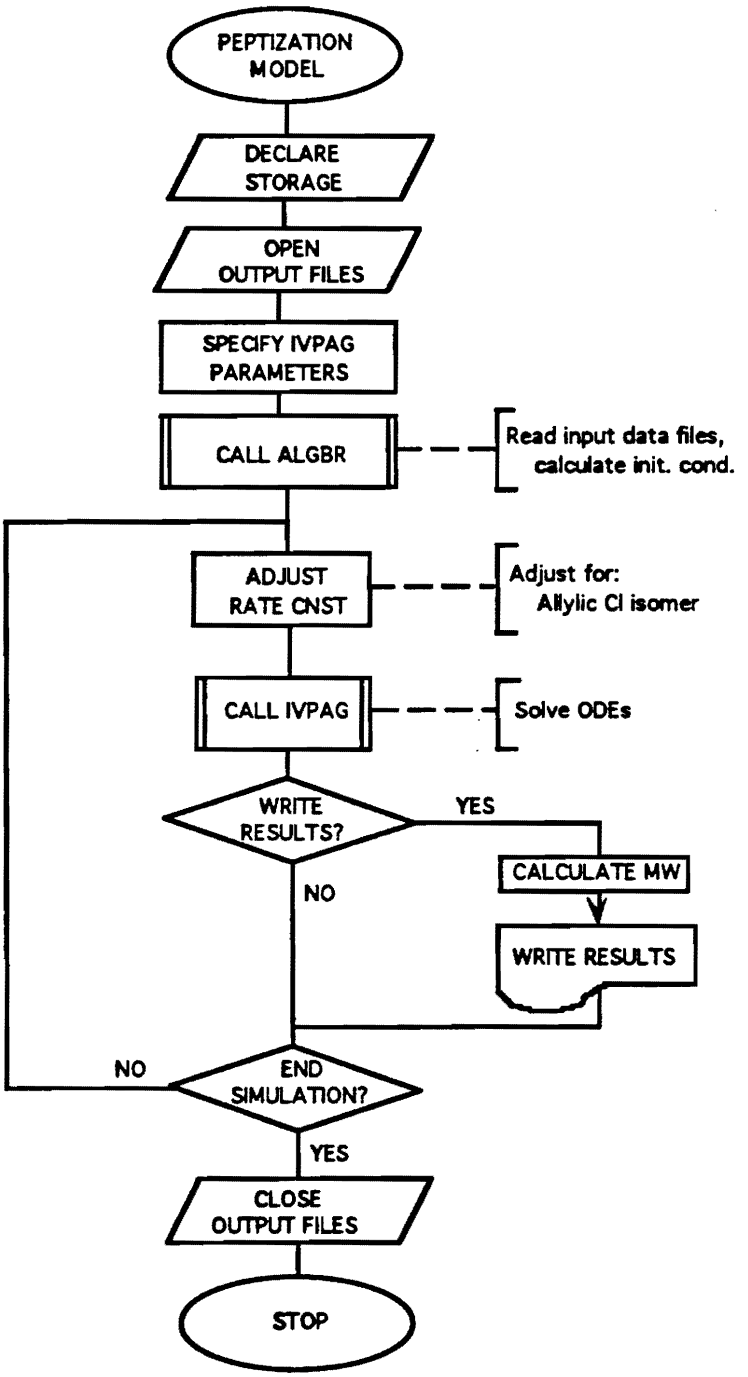

Figure 7: Peptization Model Flowchart

Table 7: Rate Constant Estimates[6]

Rate Constant	Value, $l/mol-sec$		Temp., °C
	CH_3CN/H_2O	CH_2Cl_2	
k_1	19	10^{-2}–10^{-4}	22
k_1	49	—	40
k_2	76	—	21
k_3	0.19	10^{-2}	23
k_3	0.49	—	40
k_6	60	10–10^2	21
k_7	$\sim 10^{-6}$	—	20
k_7	1.2×10^{-4}	—	78

Table 8: Arrhenius Parameters

	$\left(\frac{E}{R}\right), K$	$A, cc/molsec$
k_1	4866.	2.75E11
k_2	4594.	4.62E11
k_3	5169.	7.22E09
k_6	4603.	3.75E11
k_7	8498.	3.88E09

medium polarity effects appear significant, rate constant measurements using swollen and unswollen particles revealed an insensitivity of the rate of diffusion of small molecules (*e.g.* Tepidone, TETD) to the degree of swelling[6]. Thus, Reactions 1 and 6 are probably less affected by medium viscosity than are Reactions 2, 3, and 7, which involve two macromolecules. The model allows for independent adjustment of the constants for medium polarity and viscosity effects (RMEDCOR parameters).

Still another adjustment is made to k_3, the rate constant characterizing the branching reaction at the allylic chloride. Arthur[6] was unable to synthesize a pure sample of the tertiary allylic chloride, so the reported k_3 applies to the primary isomer. The respective rate constants may differ by 5X (tertiary more reactive). However, by the time 30% of the tertiary isomer has reacted, the remainder has rearranged to the primary isomer. Thus, Model I multiplies k_3 by 5 until 30% of the allylic chloride sites are branched, at which point the adjustment ceases.

The final rate constant adjustment is made to accommodate an apparent reduction in the reactivity of the polysulfide linkages as peptization progresses and the overall sulfur rank is reduced. This is consistent with the presence of residual cleavable sites in the peptized rubber. Arthur[6] quantified this reduction by measuring k_1 with di-, tri- and tetrasulfide in CH_3CN/H_2O at 22°C.

Sulfur Rank	k_1, $l/mol - sec$
2	3.3E-04
3	6.4E-02
4	2.0E+01

By inference, k_1 for S_6 is probably on the order of 10^2, and is reduced by 2 or 3 orders of magnitude when S_6 is cleaved to a linkage of lower rank. In the model, k_1 and k_2 are multiplied by a user-specified reduction factor (RKRED) in rate expressions for lower sulfur rank linkages.

In addition to rate constant estimates, Arthur[6] also reports useful mass transfer-related data. The Tepidone partition coefficient is estimated at 1/150, and Tepidone uptake data (t vs. T_w) is reported for several Neoprene GRT latexes. Using this data, Schork[11] estimated k_m, the mass transfer coefficient, at 6.4E-10 cm/sec.

IV. Simulation Results

A. Comparison with Laboratory Data

G Neoprene peptization sample sets, prepared and analyzed by Gossen and Aronson[3], were used to further improve the rate constant, and other model parameter, estimates. Experimental details are reported separately[3]; conditions are summarized in Table 9. Weight-averaged particle diameters were calculated from light transmission data according to D_p = 117 - 1.68(%trans), as reported by Aronson[5]. The runs basically involved aging unstripped G Neoprene plant or miniworks latex samples under controlled laboratory conditions. With the exception of Run 3, the aging temperature was maintained at 40°C, but Tepidone and TETD concentrations were intentionally varied. Samples were analyzed for MWD (GPC in THF), residual TETD, Mooney viscosity, and various other data. Standard Neoprene GW and GRT recipes are presented in Appendix II, along with some analytical results for each of the six sample sets. Use of the data to improve model parameter estimates is presently discussed.

Table 9: Summary of Peptization Experiments[3]

Run #	Polymer Type	Conv. %	D_p, nm	Sulfur, g phm	Pep. T, °C	TETD, g phm	Tepidone N, g phm
(Standard)	GW	—	—	0.335	40	1.1800	2.0000
(Standard)	GRT	83–85	95–100	0.600	40	0.4348	0.7990
1	GWM2	71.3	90.1	0.335	40	1.1800	0.7976
2	GRT	—	—	0.600	40	0.4468	0.8505
3	GRT	82.2	—	0.600	30	0.4815	0.8505
4	GRTM2	84.7	93.5	0.600	40	0.3451	1.3607
5	GWM2	70.8	102	0.335	40	1.1800	2.1300
6	GRTM1	84.4	102	0.600	40	0.5519[a]	2.2547

[a]2nd shot added after 24 hrs = 1.3015.

Molecular weight profiles of the laboratory sample sets are shown in Figure 8 (data in Table A.II.1). To aid discussion, the peptization reactions, rate constant order of magnitudes, and probable correction factors are summarized in Table 10. In Table 10, the reaction rate order of magnitude (from Table 7) is multiplied by factors estimating the difference between the polarity and viscosity of acetonitrile/water and the particle interior. A sulfur rank adjustment is also included because k_1 and k_2 were measured using an S_4 model compound[6], and the more reactive S_6 is presumed prevalent in the unpeptized polymer.

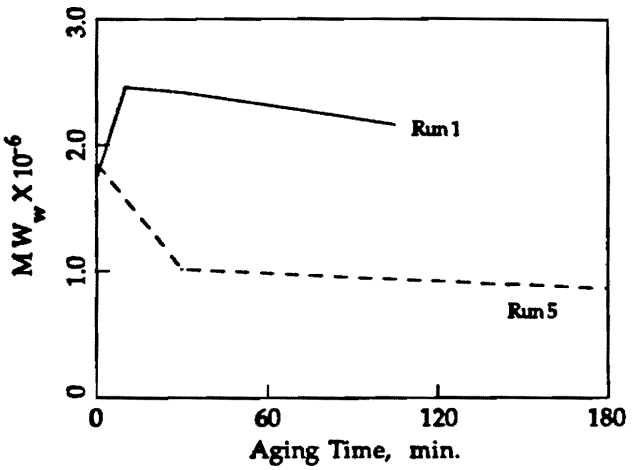

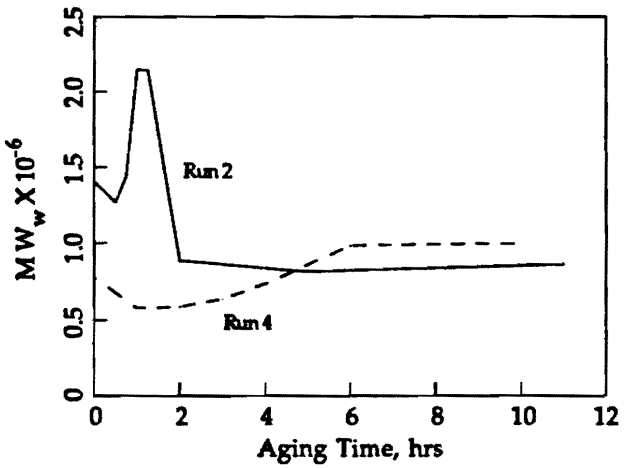

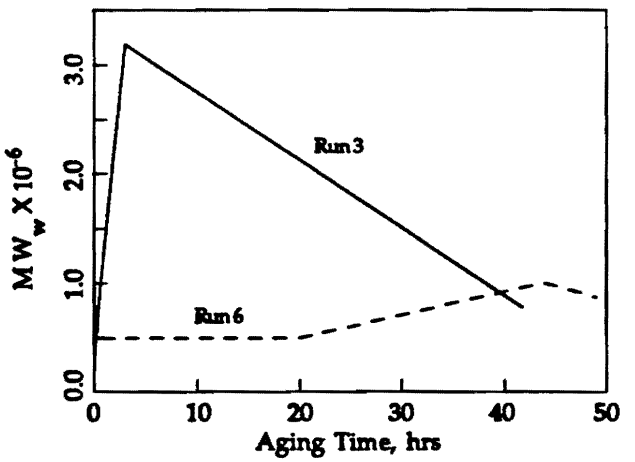

Figure 8: GW and GRT Experimental MW_w Profiles[3].

Table 10: Peptization Rate Constants

Peptization Reaction	k_i, cc/mol-sec (in CH_3CN/H_2O, 20°C)	Rate Adjustments			k_i, cc/mol-sec (in particle, 20°C)
		Polarity	Visc	S Rank	
$M_n + T^- \xrightarrow{k_1} S^-M_q + M_{n-q}T$	O(10^4)	10^{-3}–10^{-5}	1	10	O(1–10^2)
$M_n + S^-M_q \xrightarrow{k_2} M_r + S^-M_m$	O(10^4)	10^{-3}–10^{-5}	10^{-1}	10	O(10^{-1}–10)
$M_n + S^-M_q \xrightarrow{k_3} M_{n+q} + Cl^-$	O(10^2)	10^{-1}	10^{-1}	1	O(1)
$TT + S^-M_q \xrightarrow{k_4} T^- + TSM_q$	O(10^4)	1–10	1	1	O(10^4–10^5)
$M_n + S^-M_q \xrightarrow{k_7} M_{n+q} + Cl^-$	O(10^{-3})	10^{-1}	10^{-1}	1	O(10^{-5})

The corrected constants suggest that 1) reaction at the vinyl chloride sites (Reaction 7) is relatively insignificant, and 2) the reaction of TETD with polymeric sulfide ions is *very* fast. The potential dominance of Reaction 6 is of particular importance since this capping reaction is thought to deter MW increases. Note, however, that the rate of the branching (MW-increasing) and capping reactions are obviously also dependent upon the allylic Cl and TETD concentrations. At the beginning of a standard GRT peptization, the allylic Cl site concentration is roughly 3 orders of magnitude greater than the TETD concentration (calculated from the recipe in Appendix II). Therefore, as peptization continues, concentration differences could offset the disparity in rate constants, allowing a MW increase. This is possibly the case in Runs 4 and 6, where residual TETD is present (by titration), but the MW eventually increases.

Runs 4 and 6 do not, however, exhibit the large MW increases during the early stages of peptization observed in the Run 1, 2 and 3 sample sets. As discussed earlier (Section II.A.), the extent of this increase appears to be related to the unpeptized polymer structure[3]. Polymer characterized by a persistent multimodal MWD with a preponderance of low MW chains exhibit a larger, more sustained MW increase during the early stages of peptization (Runs 1, 2, and 3). Model I does not accommodate multimodal MWDs and therefore does not predict this early MW increase. Similarly, several sample sets exhibited a significant change in MW with the addition of TETD only (Table 3). The Model I mechanism requires Tepidone for the onset of peptization, but is still useful if a continued MW increase does not ensue. Run 4 simulations are presented first.

In Run 4, the standard recipe TETD and Tepidone charges are decreased by 20% and doubled, respectively, to force an increase in Mooney viscosity with peptization time. Simulations are shown in Figures 9 and 10. Rate constant correction factors are summarized in Table 11 (k_7 is omitted, but was adjusted in the same manner as k_3). The required corrections for k_1, k_2, and k_3 were in the expected ranges, but k_6 was reduced further to obtain a reasonable fit to the MW_w data (Figure 9a). This is consistent with the substantial ($\sim$ 50%) residual TETD level (Figures 9b and 10a). With a very high k_6, the MW continued to decrease despite the high allylic Cl concentration (Figure 10b). The residual aqueous-phase Tepidone concentration is also substantial ($\sim$ 60%, Figure 10a), and the particle-phase concentration is relatively low (Figure 10c). This aqueous phase preference is consistent with the estimated Tepidone partition coefficient[6]. Returning to Figure 10b, note that the more reactive S_6 linkage level is plotted. As these are cleaved, less reactive sites remain. Polydispersities (not shown) were higher than expected, possibly reflecting the unimodal MWD assumption or the need for further k_2 adjustment.

Table 11: Rate Constant Correction Factors

Constant	Run 4	Run 6	Run 2	Run 5
k_1	4.00E-02	3.00E-02	3.00E-02	3.00E-02
k_2	3.00E-03	3.00E-03	3.00E-03	3.00E-03
k_3	3.15E-02	3.30E-02	3.30E-02	8.75E-02
k_6	2.50E-03	2.00E-03	2.00E-03	2.00E-03

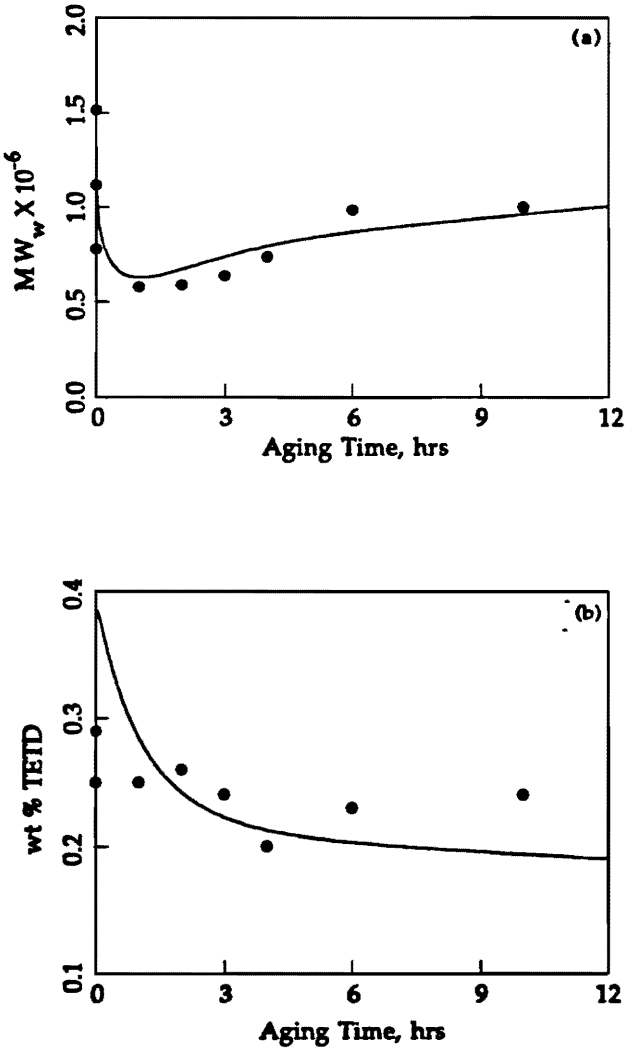

Figure 9: Model Fit to Run 4 MW_w and wt% TETD.

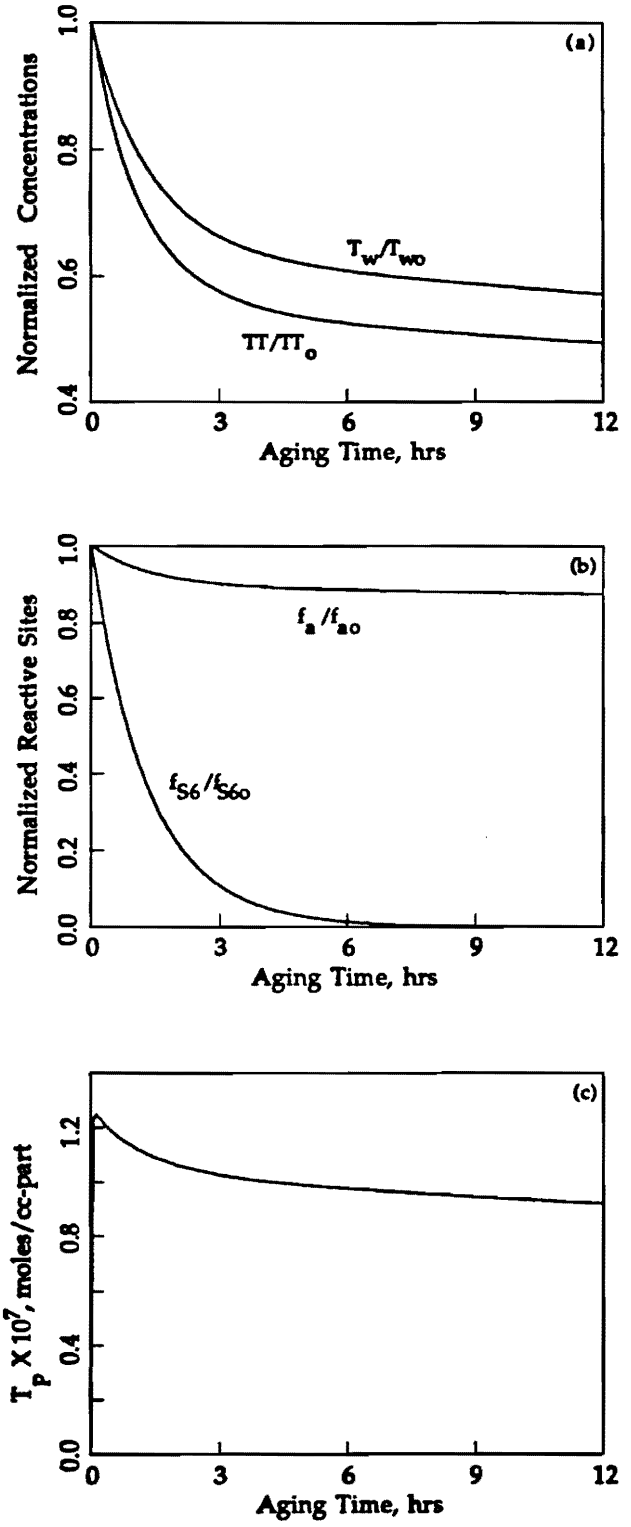

Figure 10: T_w, TETD, Reactive Site and T_p Predictions (Run 4)

Run 6 tracked a 'GRTM1' (a GW Tepidone charge was inadvertantly added) peptization over 3 days. Additionally, a second TETD shot was added to some samples after 24 hours. Simulations are shown in Figures 11 and 12. With only slight adjustment of the rate constants used for Run 4 simulations (Table 11), a reasonable MW_w fit is obtained (Figure 11a) and an impressive wt% TETD prediction is noted (Figure 11b). Consistent with the proposed reaction mechanism, the second TETD shot reverses the MW increase by capping chains that would otherwise be coupled. Figure 12 shows the expected decrease in the rate of allylic Cl depletion.

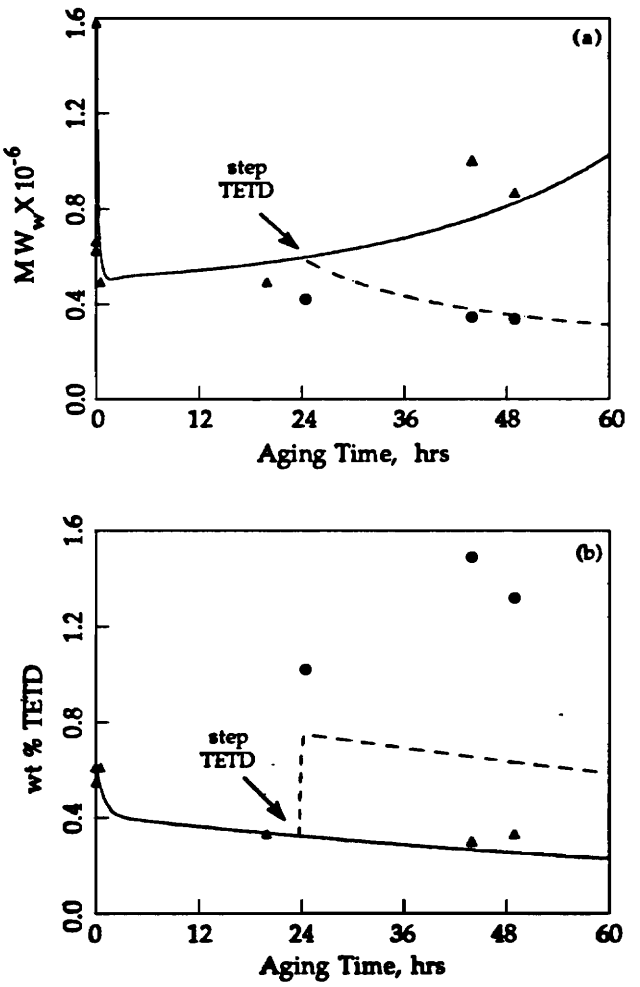

Figure 11: Model Fit to Run 6 MW_w and wt% TETD.

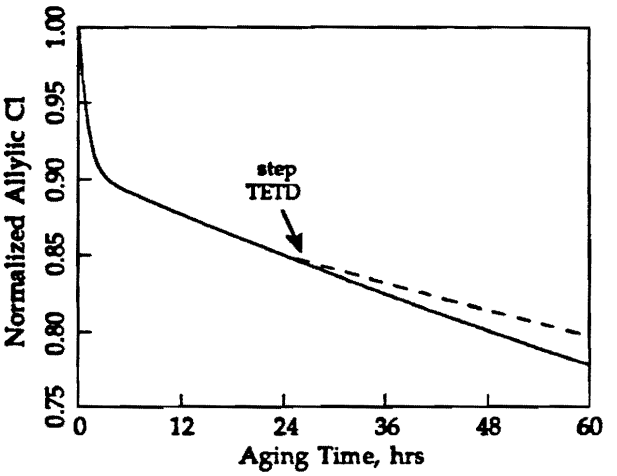

Figure 12: Allylic Cl Prediction (Run 6)

In Run 2, a standard GRT peptization, MW_w doubled during the first hour of peptization, presumably reflecting polymer structural changes associated with the transition from a multimodal to unimodal MWD. Model I does not accommodate these changes, but simulation of the subsequent MW_w decrease is shown in Figure 13. Here, the *aged* polymer properties were used as initial conditions. The initial Tepidone and TETD concentrations were not adjusted since T_p quickly assumes a low value, and a substantial TETD residual was measured. Allylic Cl and polysulfide site concentrations were likewise unadjusted since the structural reconfiguration chemistry has not been identified.

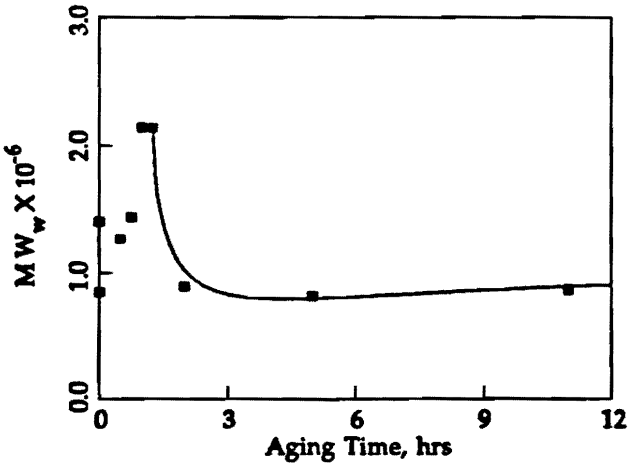

Figure 13: Model Fit to Run 2 MW_w.

Lastly, Run 5 tracked a standard GW peptization for 3 hours. While the unpeptized polymer MWD was not perfectly unimodal, MW_n was not extremely low and a smooth MW_w decrease was measured. A good fit of the data was obtained (Figure 14a) by more than doubling k_3, the rate constant for branching at the allylic Cl (Table 11). A corresponding increased allylic Cl depletion is not predicted (Figure 14b). The correctness of this k_3 increase should be weighed in light of GW and GRT polymer differences.

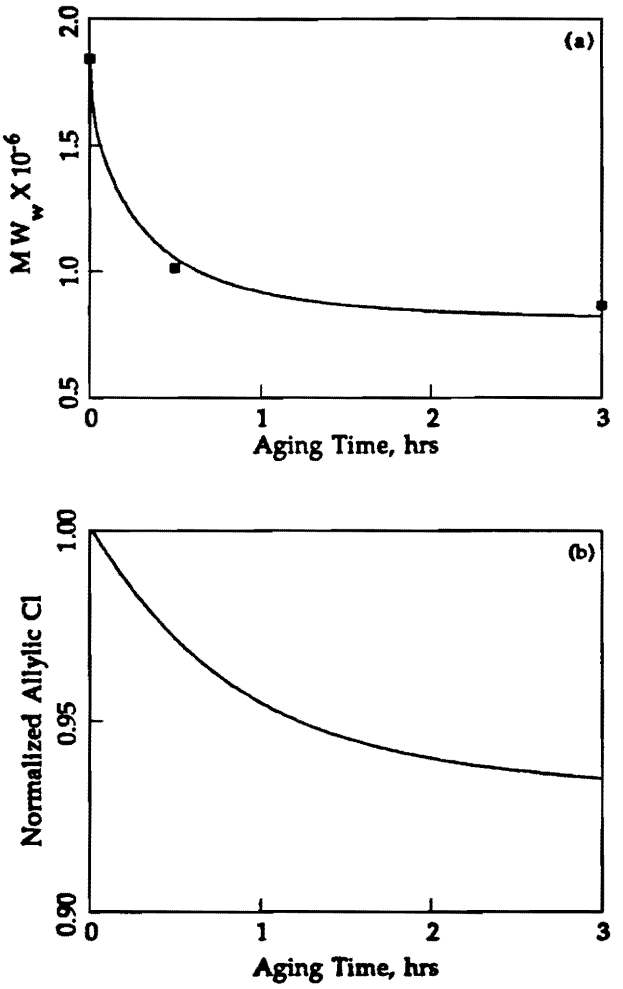

Figure 14: Model Fit to Run 5 MW_w, Allylic Cl Prediction.

B. Sensitivity Analysis

The sensitivity of Model I predictions to the reaction rate constants (k_1, k_2, k_3, k_6), recipe parameters (Tepidone, TETD, sulfur incorporation), the rate reduction factor, and mass transfer parameters (Tepidone partition coefficient, k_m, D_p) is evaluated by changing the subject parameter, while leaving the others unchanged. (Alternatively, one might employ a rigorous statistical procedure, e.g. ANOVA, for further detail.) The standard GRT recipe, with Run 4 rate constant correction factors, is used as the base condition.

Sensitivity of the MW_w predictions to $\pm 50\%$ changes in k_1 and Tepidone concentration is shown in Figure 15. Consistent with Reaction 1, increasing k_1 or the Tepidone concentration increases the rate at which polysulfide linkages are cleaved, and thus the MW_w reduction rate. Since this is a rate effect, a comparable MW is reached, sooner or later, in all cases. However, acceleration or deceleration of this rate similarly affects the onset of an observable MW increase due to branching.

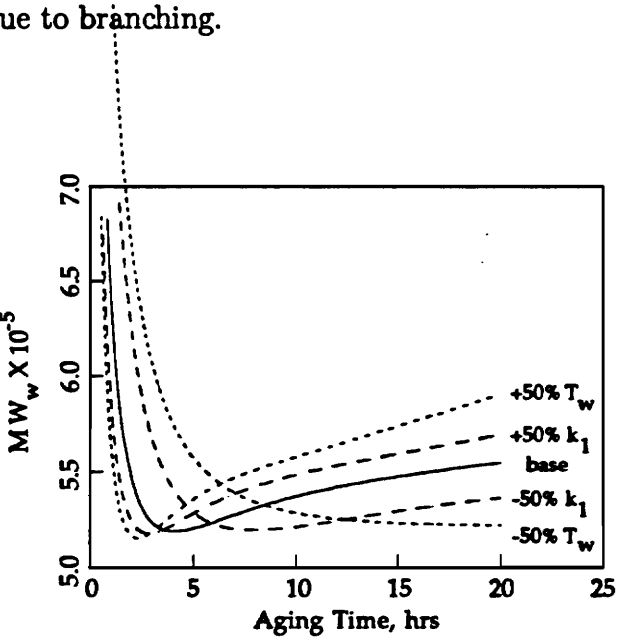

Figure 15: Model Sensitivity to k_1 and [Tepidone].

With fixed rate constants, the minimum predicted MW varies with sulfur incorporation (Figure 16). Although not verified quantitatively, the scale of this variance appears consistent with incorporated sulfur versus Mooney viscosity data reported by Aronson[5]. Less incorporated sulfur results in fewer polysulfide linkages, the cleavable sites affording MW reduction, and higher final MW levels.

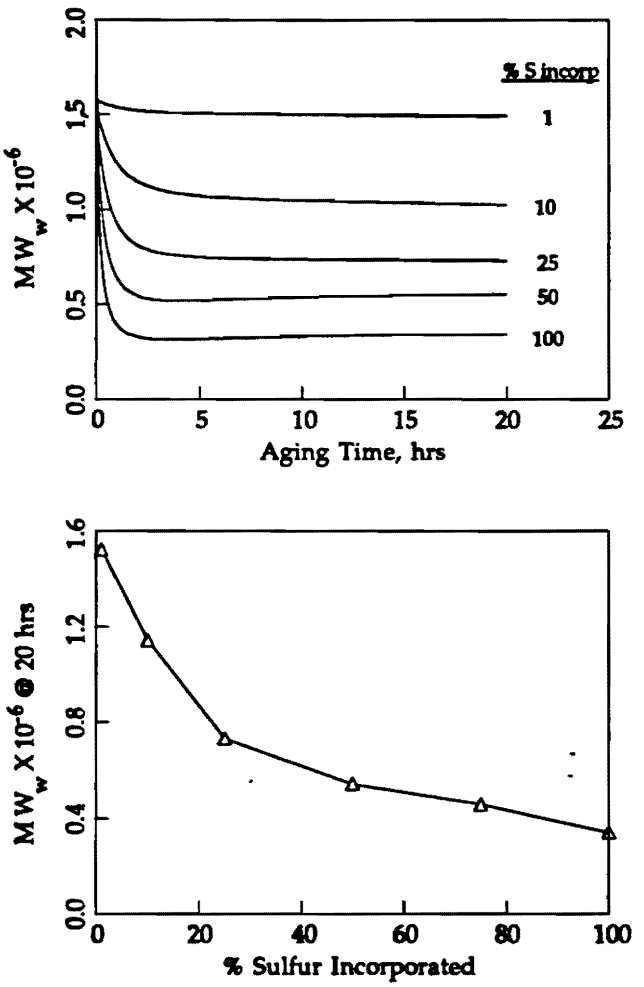

Figure 16: Model Sensitivity to Sulfur Incorporation.

MW profiles are also sensitive to k_3 and k_6, the rate constants governing the branching (allylic Cl) and capping reactions. As shown in Figure 17, and explained by the proposed mechanism, increasing k_3 increases the likelihood that a polymeric sulfide ion will be branched via Reaction 3, rather than redistributed (Reaction 2) or capped (Reaction 6). Note that MW does not increase when k_3 and TETD are increased simultaneously (Figure 17a). However, the MW increase is accelerated with significant decreases in either k_6 or TETD (Figure 17b) since polymer chains are again more likely to be branched than capped.

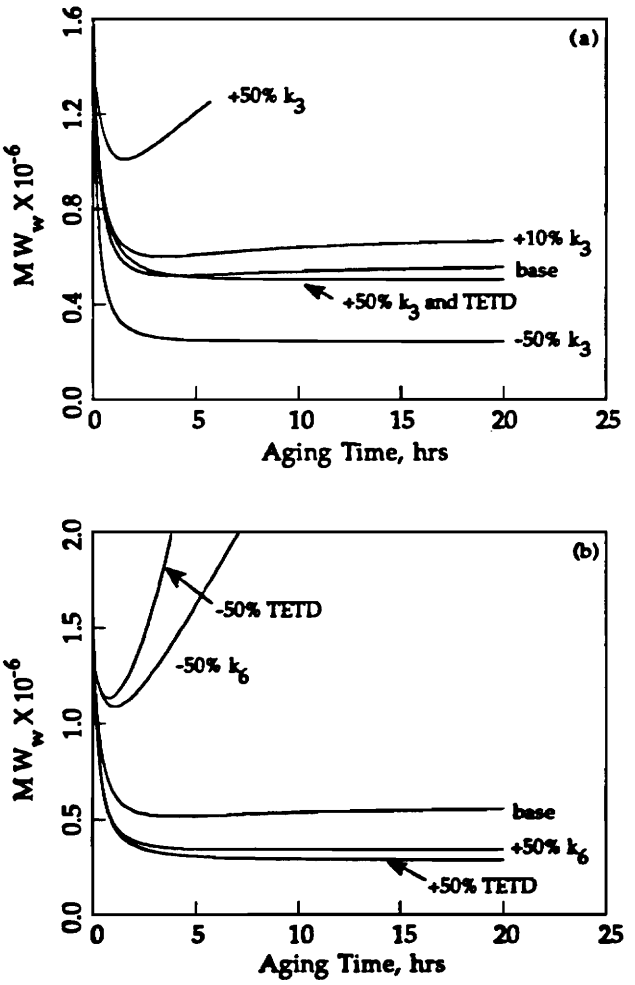

Figure 17: Model Sensitivity to k_3, k_6 and [TETD].

Consistent with the proposed mechanism, adjusting k_2, the rate constant characterizing the MW redistribution reaction, appears to affect the final MW attained, but not the MW reduction rate (Figure 18). Increased redistribution appears to lower both the MW_w and polydispersity. This is noted in light of the model equations, which suggest that Reaction 2 can decrease or increase MW depending on the polymer chain (M_n) and polymeric sulfide ion (S_n) distributions (Section II.D.). The polydispersity profile is unexpected and may reflect the unimodal MWD assumption.

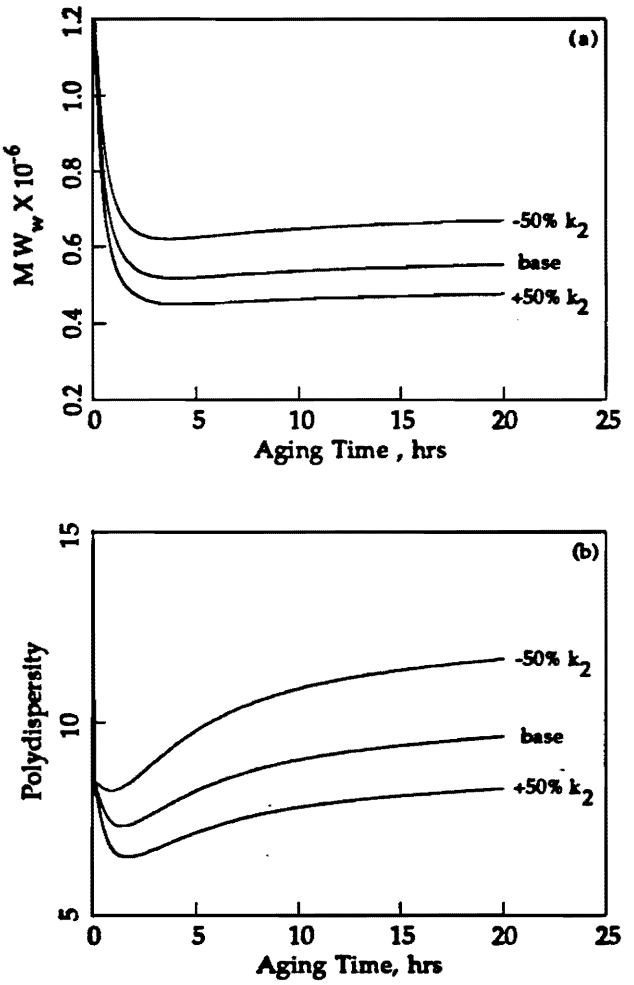

Figure 18: Model Sensitivity to k_2.

Both k_2 and k_1 are corrected for the continued reduction of S_6 linkages to S_2, S_3 and/or S_4 sites, whose reactivity is reduced by at least 2 to 3 orders of magnitude. Adjusting this parameter (RKRED, from base 10^{-2} and 10^{-3}) does not significantly affect the early aging curve, when S_6 sites are relatively plentiful. However, when the S_6 sites are nearly depleted, decreasing RKRED can virtually halt all reactions in the Model I mechanism. Specifically, if Reaction 1 does not proceed, the polymeric sulfide ions (S_n) required for Reactions 2, 3 and 6 are not formed, and all reactions cease. This is depicted in Figure 19, where the MW increase observed during Run 6 is not predicted if RKRED is reduced by an order of magnitude (to 10^{-3}).

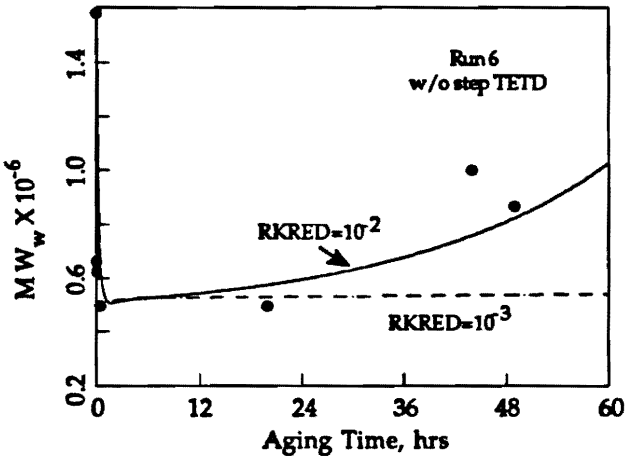

Figure 19: Model Sensitivity to RKRED.

Lastly, consider model sensitivity to mass transfer parameters. Of the three parameters considered (Tepidone partition coefficient, k_m, and D_p), only the particle diameter does not significantly affect the peptization rate. The Tepidone partition coefficient (PC) was estimated at $\frac{1}{150}$[6], but could be as low as $\frac{1}{1000}$ or as high as $\frac{1}{10}$[11]. As shown in Figure 20a, decreasing PC by an order of magnitude decreases T_p by roughly 90%, and lowers the peptization rate (Figure 20b). On the other hand, increasing PC by an order of magnitude accelerates the process to the extent that an early MW increase (due to branching) is observed. TETD depletion is accelerated (Figure 20c), with an ensuing reduction in the capping reaction rate.

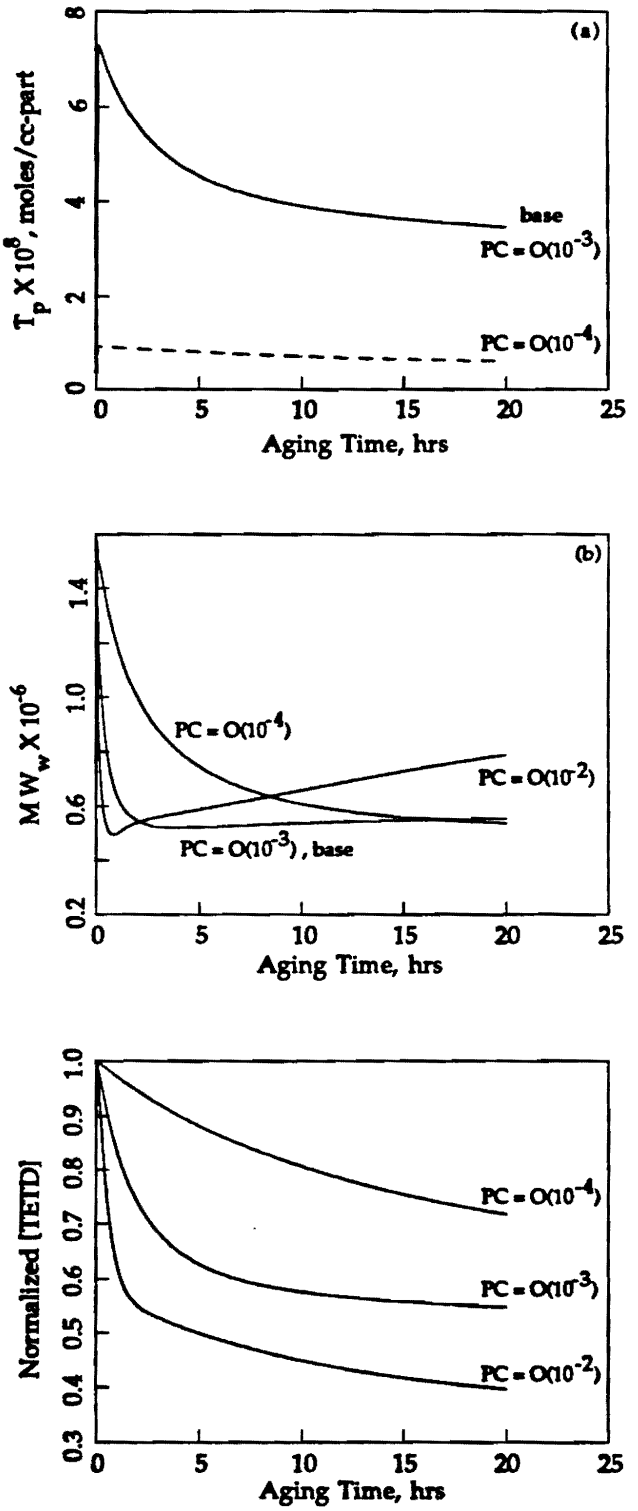

Figure 20: Model Sensitivity to Tepidone Partition Coefficient(PC).

Order of magnitude changes in k_m, the mass transfer coefficient, significantly affect peptization, but $\pm 20\%$ changes in D_p, the weight-averaged particle diameter, do not significantly affect Tepidone transfer (Figure 21). A smaller particle and/or larger k_m increases T_p and thus accelerates the MW reduction, and vice versa, but, in the case of D_p, these effects are negligible. Thus, the increase in Mooney viscosity with particle size observed in practice is not fully explained by Tepidone mass transfer. Note, however, that changing *either* k_m *or* D_p by an order of magnitude has the same effect on T_p predictions (Eqn. (20), $\frac{k_m a_p}{v_p} = \frac{k_m 6}{D_p}$ for spherical particles). Thus the predicted particle size effect could be more significant for very polydisperse latexes.

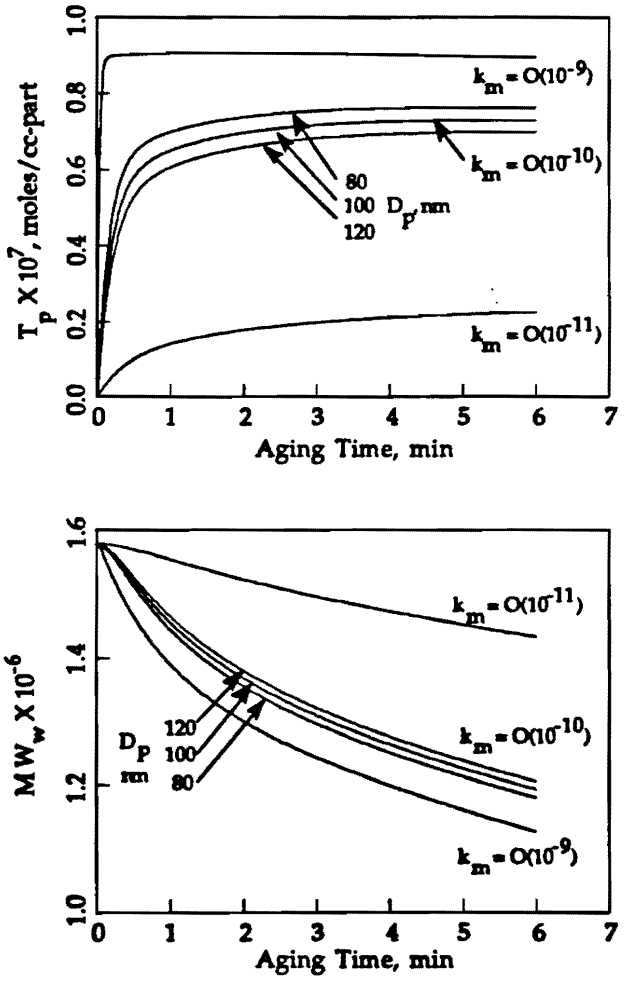

Figure 21: Model Sensitivity to k_m and D_p.

C. Predictive Capability

Doyle's study of Mooney viscosity for Neoprene G types[7] provides useful data for independent assessment of the model predictive capability. Doyle measured aging curves (Mooney viscosity versus time) at 25°C for a wide range of TETD and Tepidone concentrations. While Mooney viscosity is not totally indicative of MWD (Figure 22), a general correlation appears valid (Figure 23), and was used to convert Doyles's aging curves to approximate MW_w profiles. In the simulations that follow, the unpeptized polymer is assumed similar to that of Run 6, as are the rate constants.

Figure 24 shows the effect of varying the Tepidone level at a fixed TETD concentration. As expected, Mooney viscosity and MW_w decrease with increased Tepidone concentration according to Reaction 1. Consistent with Reaction 6, at a fixed Tepidone level, MW_w decreases with increased TETD concentration (Figure 25), as more chains are capped rather than branched. Mechanistically, fixing the TETD/Tepidone ratio *balances* the capping (and thus branching) and scission reactions.

Finally, in Figure 26, both the model predictions and experimental aging curves exhibit the expected increase in peptization rate with increased temperature. This is consistent with the representation of the rate constants by Arrhenius' law.

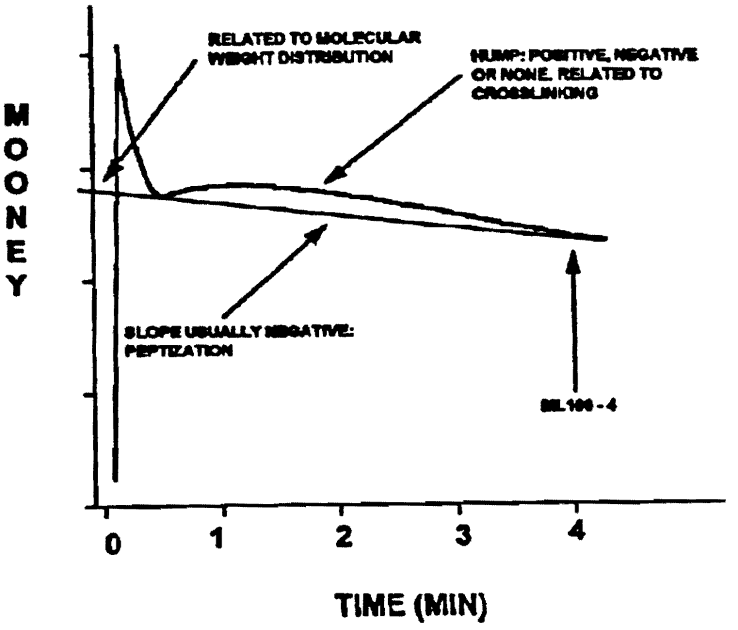

Figure 22: Mooney Curve.

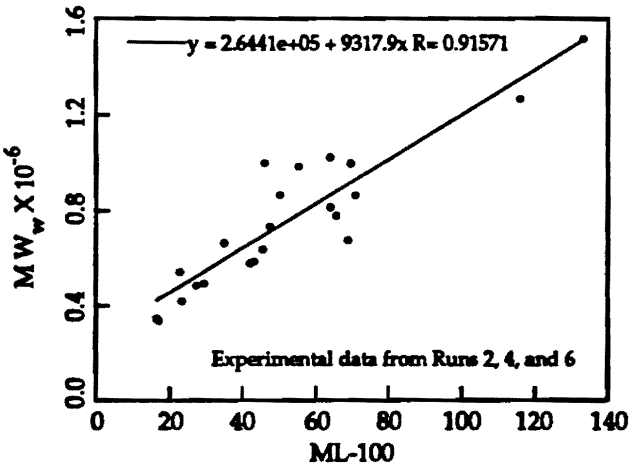

Figure 23: Mooney/MW Correlation.

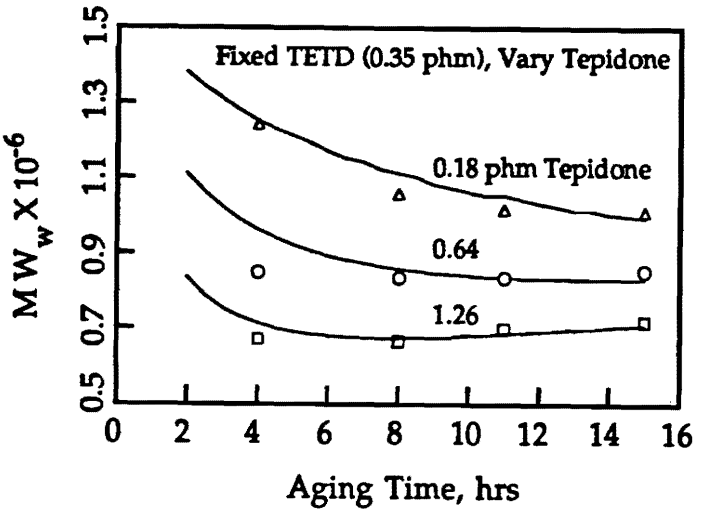

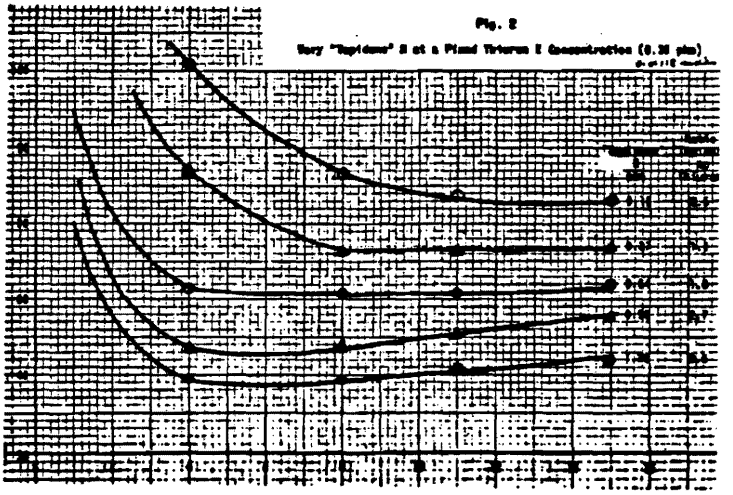

Figure 24: Model Comparison with Mooney Trends[7]: Constant $TETD$, Vary T^{-}.

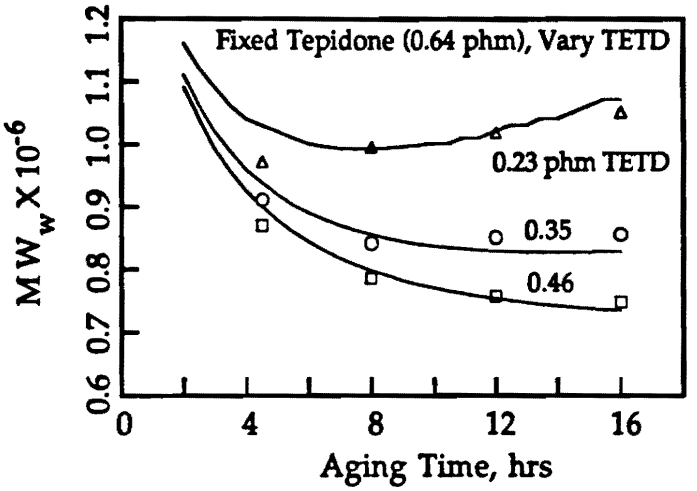

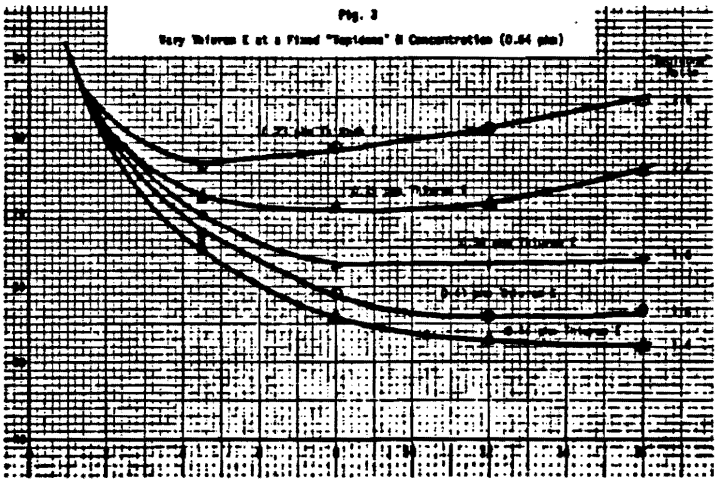

Figure 25: Model Comparison with Mooney Trends[7]: Constant T^-, Vary *TETD*.

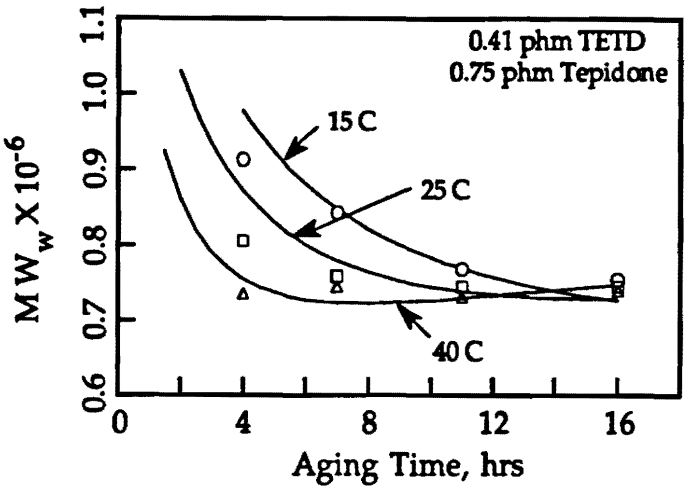

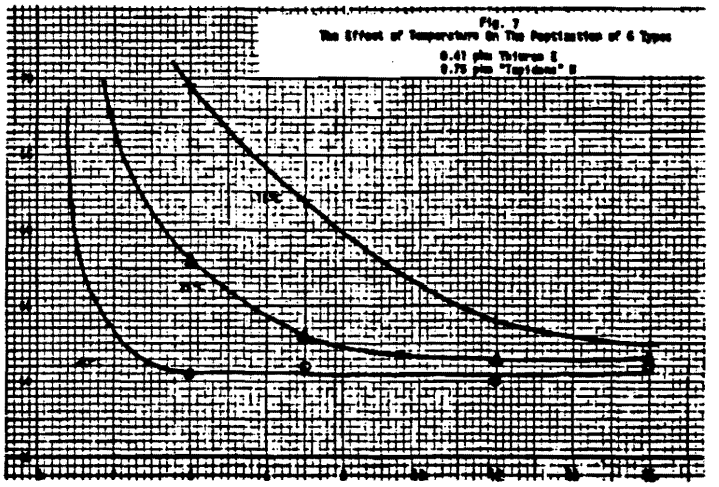

Figure 26: Model Comparison with Mooney Trends[7]: Temperature Effect.

References

[1] F.J. Schork, 'G-Type Neoprene Latex Aging', August 2, 1991.

[2] C.L. Liotta and F.J. Schork, 'G-Type Neoprene Latex Aging Proposed Mechanistic Studies', January 5, 1992.

[3] P. Gossen and M. Aronson, 'G-Neoprene Peptization: Advances in Understanding the Evolution of Polymer Microstructure', DP 93-L-3.

[4] H.E. Simmons III, Peptization Meeting Presentation, March 30, 1993.

[5] M. Aronson, Peptization Meeting Presentations, Georgia Institute of Technology, November 10, 1992, March 30, 1993.

[6] S. Arthur, 'Neoprene Peptization Kinetics Derived from Model Compounds', DP 92-E-35.

[7] A.M. Doyle, 'Improved Mooney Viscosity Control for Chloroprene-Sulfur Copolymers (Neoprene G Types)', ERD-3401.

[8] W.H. Ray, 'On the Mathematical Modeling of Polymerization Reactors', *J. Macromol. Sci. - Revs. Macromol. Chem.*, C8(1), 1-56(1972).

[9] F.J. Schork, *Control of Polymerization Reactors*. New York, NY: Marcel Dekker, 1993.

[10] M.V. Tirrell and R.L. Laurence, 'Polymerization Reaction Engineering,' notes for a short course at the University of Minnesota Polymerization and Polymer Process Engineering Center, Minneapolis, MN, 1983.

[11] F.J. Schork, 'Mass Transfer Effects in GRT Tepidone Uptake', December 7, 1992.

APPENDIX I

Nomenclature[1]

a_p	surface area of a particle, $cm^2/particle$
A_p	total surface area of particles, $cm^2 - particle$
$[AC]$	allylic chloride concentration, $moles/cc - part$
f_a	fraction allylic chlorides in polymer chain, $moles/mole\ mer$
f_s	fraction polysulfide linkages in polymer chain, $moles/mole\ mer$
f_v	fraction vinyl chlorides in polymer chain, $moles/mole\ mer$
k_i	rate constant for Reaction i, $cc/mole\ sec$
k_m	mass transfer coefficient, cm/sec
M_n	polymer of chain length n, $moles/cc - part$
MW_n	number-average molecular weight, $g/mole$
MW_w	weight-average molecular weight, $g/mole$
$[RS]$	polysulfide reactive site concentration, $moles/cc - part$
S^-M_n, S_n	polymeric sulfide ion of chain length n, $moles/cc - part$
T^-	dithiocarbamate (ethyl or butyl), $moles/cc$
T_p	Tepidone in particle, $moles/cc - part$
T_w	Tepidone in aqueous phase $moles/cc - aq$
$TETD, T_eT_e$	tetraethylthiuram disulfide, $moles/cc - part$
T_bT_b	tetra n-butyl thiuram disulfide
T_eT_b	diethyldibutylthiuram disulfide
TT	thiuram disulfide (ethyl, butyl, or mixed), $moles/cc - part$
v_p	volume of a particle, $cc/particle$
$[VC]$	vinyl chloride concentration, $moles/cc - part$
V_w	aqueous-phase volume, $cc - aq$
w	monomer molecular weight, $g/mole$
$\mathcal{M}(z)$	z-transform of M_n
$\mathcal{S}(z)$	z-transform of S_n
η_i	ith moment of M_n distribution
λ_i	ith moment of S_n distribution

[1]See Appendix III for computer variable notation.

APPENDIX II

Neoprene GW Recipe

	parts per 100 Monomer
Monomer Solution	
Chloroprene	100.0
Rosin S	4.0
Water Solution	
Demineralized water	93.97
Copper Ion	0.4 ppm
Sodium Hydroxide(50%)	1.26
Sodium Chloride	0.075
Sulfur Dispersion	
Sulfur	0.335
20% 'Lomar' PW	1.75
Catalyst Solution (A-3)	
Demineralized water	1.613
Potassium persulfate	0.085
Silver salt	0.0021
Kettle Stabilizer (Type V)	
Toluene	1.634
Demineralized water	1.227
Dresinate X	0.034
TETD	1.180
'Ethyl' Antioxidant 736	0.047
'Duponol' WAQE	0.167
Kettle Plasticizer	
'Tepidone' N	2.0
'Duponol' WAQE	0.13

Model Parameters

DPART	1.1206
GTEPN	2.00
GTETD	1.180
GSUL	0.335
VW	101.8
WP	107.71

Neoprene GRT Recipe

	parts per 100 Monomer
Monomer Solution	
Chloroprene	98.0
ACR	2.0
Rosin S	4.0
Water Solution	
Demineralized water	105.77
Copper Ion	0.4 ppm
Sodium Hydroxide(50%)	1.40
Sodium Chloride	0.075
Sulfur Dispersion	
Sulfur	0.6
20% 'Lomar' PW	3.0
Catalyst Solution (A-3)	
Demineralized water	4.270
Potassium persulfate	0.225
Silver salt	0.0056
Kettle Stabilizer (Type I)	
Toluene	0.6325
Demineralized water	0.6031
Dresinate X	0.0150
TETD	0.4348
Santowhite Crystals	0.0925
'Duponol' WAQE	0.0721
Kettle Plasticizer	
'Tepidone' N	0.799
'Duponol' WAQE	0.051

Model Parameters	
DPART	1.1603
GTEPN	0.799
GTETD	0.4348
GSUL	0.6
VW	115.33
WP	106.64

Table 12: Laboratory Peptization Sample Data*[3]

Aging Time	MW_n	MW_w	PD	TETD, wt%
Run 1 (GWM2)				
before $T^-, TETD$	184,000	1,736,000	9.4	—
10 min.	136,000	2,459,000	18.1	—
30 min.	184,000	2,415,000	11.0	—
105 min.	171,000	2,158,000	12.6	—
Run 2 (GRT)				
before $T^-, TETD$	108,000	854,000	7.9	0.10
after $TETD$, before T^-	105,000	1,408,000	13.4	0.26
30 min.	104,000	1,269,000	12.2	0.36
45 min.	108,000	1,441,000	13.4	0.31
60 min.	121,000	2,143,000	17.7	0.26
1.25 hr	128,000	2,141,000	16.7	0.26
2.00 hr	96,000	891,000	9.3	0.29
5.00 hr	100,000	815,000	8.1	0.25
11.00 hr	102,000	865,000	8.5	0.18
Run 3 (GRT)				
0 min.	24,000	331,000	13.9	—
30 min.	66,000	932,000	14.1	—
3 hr	159,000	3,191,000	20.0	—
41.75 hr	118,000	774,000	6.5	—
Run 4 (GRTM2)				
before $T^-, TETD$	109,000	1,119,000	10.3	—
after $TETD$, before T^-	—	1,516,000	—	0.29
0 hr	91,000	780,000	8.6	0.25
1 hr	116,000	579,000	5.0	0.25
2 hr	—	587,000	—	0.26
3 hr	—	638,000	—	0.24
4 hr	—	735,000	—	0.20
6 hr	—	985,000	—	0.23
10 hr	103,000	1,000,000	9.8	0.24
Run 5 (GWM2)				
before $T^-, TETD$	236,000	1,844,000	7.8	0
30 min.	142,000	1,011,000	7.1	1.24
3 hr	136,000	861,000	6.3	1.24
Run 6 (GRTM1)				
before $T^-, TETD$	105,000	1,579,000	15.0	0
after $TETD$, before T^-	114,000	625,000	5.5	0.55
0 hr	106,000	664,000	6.3	0.61
0.5 hr	102,000	495,000	4.9	0.61
20 hr	84,000	495,000	5.9	0.33
44 hr	89,000	1,001,000	11.2	0.30
49 hr	99,000	866,000	8.7	0.33
24.5 hr w/2nd TT	—	421,000	—	1.02
44 hr w/2nd TT	79,000	344,000	4.4	1.49
49 hr w/2nd TT	71,000	336,000	4.7	1.32

*MW measured by GPC(THF), TT measured by titration.

Appendix III

Computer Program

A. Variable Notation (underlined variables are required input)

A(1,1)	IVPAG parameter
Ai	frequency factor (Arrhenius' law) for RKi, *cc/mole sec*
AP	total surface area of particles, $cm^2 - part$
ALGBR	subroutine used to calculate initial conditions
CNST1.DAT	input data file
DCM	weight-average particle diameter, *cm*
IVPAG	IMSL subroutine used to solve ODEs
DNM	weight-average particle diameter, *nm*
DPART	particle-phase density, $g/cc - part$
DY(i)	Y(i) dummy used to facilitate data transfer
ERi	E/R (Arrhenius' law) for RKi, K
ETAi	ith moment of M_n distribution, $moles/cc - part$
ETAij	contribution of jth reaction to ETAi, $moles/cc - part\ sec$
FA	fraction allylic chlorides in polymer chain, *mole/mole mer*
FAO	initial fraction allylic chlorides in polymer chain, *mole/mole mer*
FCN	IVPAG subroutine containing ODEs
FCNJ	IVPAG subroutine containing dummy Jacobian
FCONV	fractional conversion at begin peptization
FETA	weight fraction M_n
FLAM	weight fraction S_n
FS	fraction polysulfide linkages in polymer chain, *mole/mole mer*
FSO	initial fraction polysulfide linkages in polymer chain, *mole/mole mer*
FSULINC	fraction recipe sulfur incorporated in polymer
FV	fraction vinyl chlorides in polymer chain, *mole/mole mer*
FVO	initial fraction vinyl chlorides in polymer chain, *mole/mole mer*
GSUL	sulfur, *g phm*
GSULINC	sulfur incorporated, *g phm*
GTEPN	Tepidone N, *g phm*
GTETD	TETD, *g phm*
H	IVPAG parameter
ICOUNT	count for write to output data files
IFLAG	flag to adjust RK3
INDEX	IVPAG parameter

INORM	IVPAG parameter
LAMi	*ith* moment of S_n distribution, $moles/cc - part$
MEND	number of times IVPAG called
METH	IVPAG parameter
MOLWGT.DAT	output data file
MOMENT.DAT	output data file
MXSTEP	IVPAG parameter
NODES	IVPAG parameter
PARAM(50)	IVPAG parameter
PCOUNT	write to output data files when ICOUNT=PCOUNT
RCP1.DAT	input data file
RKi	reaction rate constant for Reaction i, $cc/mole\ sec$
RKM	mass transfer coefficient, cm/sec
RKRED	factor by which RKi is reduced with S rank
RLAMij	contribution of *jth* reaction to RLAMi, $moles/cc - part\ sec$
RMEDCORi	medium polarity/viscosity correction factor
RMERMW	modified mer (chloroprene-sulfur) molecular weight, $g/mole$
RMN	MW_n of unpeptized polymer, $g/mole$
RMONMW	monomer molecular weight, $g/mole$
RMW	MW_w of unpeptized polymer, $g/mole$
RMWN	number-average molecular weight, $g/mole$
RMWW	weight-average molecular weight, $g/mole$
RNP	particle number
RPC	Tepidone partition coefficient, $(T_p/T_w)_{equil.}$
RPCOUNT	PCOUNT (real)
RPD	polydispersity of MWD
RPI	π
SAP	surface area of particle, $cm^2/particle$
SIMTIM	simulation time, *hrs*
SITES.DAT	output data file
STEPN	Tepidone N step, *g phm*
STETD	TETD step, *g phm*
SULMW	sulfur molecular weight, $g/mole$
SVP	volume of particle, $cc/particle$
T	time, *sec*
TEMP	temperature, K
TEPMW	Tepidone molecular weight, $g/mole$
TETDMW	TETD molecular weight, $g/mole$
TIDG	IVPAG parameter
TIEND	IVPAG parameter
TOL	IVPAG parameter
TSTEP	ODEs solved every TSTEP seconds during SIMTIM

TWO	initial aqueous-phase Tepidone concentration, $mole/cc - aq$
VP	particle-phase volume, $cc - part\ phm$
VW	aqueous-phase volume, $cc - aq\ phm$
WP	particle-phase weight, $g - part\ phm$
WTETD	wt% TETD (based on dry polymer)
Y(i)	dependent variable for ith ODE, $mole/sec$ Note: 1–T_w, 2–T_p, 3–TT, 4–η_0, 5–η_1, 6–η_2, 7–λ_0, 8–λ_1, 9–λ_2, 10–$[RS]$, 11–$[AC]$, 12–$[VC]$
YPRIME(i)	right-hand-side of ODE for Y(i)

B. Program Listing

```
      PROGRAM PEP

C THIS PROGRAM SOLVES MODEL I FOR G-TYPE NEOPRENE ALKALINE AGING.
C IT PREDICTS MOLECULAR WEIGHT, RESIDUAL REACTIVE SITES, AND
C PEPTIZING AGENT CONCENTRATIONS VS AGING TIME.

C DECLARE STORAGE

      DIMENSION A(1,1),PARAM(50),Y(12),DY(12)
      EXTERNAL FCN,FCNJ,IVPAG

      COMMON/MISC/ ETA3,DY,PCOUNT,RMERMW,SIMTIM,TSTEP,TWO,TTO
      COMMON/PART/ AP,RKM,RPC,SAP,SVP,VW
      COMMON/RKS/  RK1,RK2,RK3,RK6,RK7,RKRED
      COMMON/SITES/ FS,FA,FV,FSO,FAO,FVO
      COMMON/STEP/ T,TETDMW,TEPMW,VP,STETD,STEPN

C OPEN OUTPUT FILES

      OPEN(UNIT=13,NAME='MOLWGT.DAT',TYPE='NEW')
      OPEN(UNIT=14,NAME='SITES.DAT',TYPE='NEW')
      OPEN(UNIT=15,NAME='MOMENT.DAT',TYPE='NEW')

C SPECIFY IVPAG PARAMETERS

      NODES=12
      TOL=0.9E-06
      H=1.0E-10
      PARAM(1)=H
      MXSTEP=1000000000
      PARAM(4)=MXSTEP
      INORM=0
      PARAM(10)=INORM
      METH=2
      PARAM(12)=METH
      INDEX=1
      TIDG=0.0

C READ DATA FILES AND PERFORM SUPPORTING ALGEBRAIC CALCULATIONS
```

```
CALL ALGBR

DO I=1,12
Y(I)=DY(I)
ENDDO

C MAIN CALCULATION LOOP

T=0.0
ICOUNT=0
IFLAG=0
MEND=SIMTIM*3600./TSTEP

RMWN=RMERMW*Y(5)/Y(4)
RMWW=RMERMW*Y(6)/Y(5)
RPD=RMWW/RMWN
WTETD=Y(3)*TETDMW*(VP/(VP+VW))*(100./1.077)*(1./.4)

10 FORMAT (7(1X,E9.4))

WRITE(13,10) T/3600.,RMWW,RMWN,RPD,Y(1)/TWO,Y(2),Y(3)/TTO
WRITE(14,10) T/3600.,Y(10),Y(11),Y(12),FS/FSO,FA/FAO,FV
WRITE(15,10) T/3600.,Y(4),Y(5),Y(6),Y(7),Y(8),Y(9)

DO M=1,MEND
TIEND=TIDG+TSTEP
T=TIEND

C Adjust allylic chlorine rate constant

IF (IFLAG.EQ.0.AND.(FA/FAO).LE.0.70) THEN
RK3=RK3/5.0
IFLAG=1
ENDIF

C Solve ODEs

CALL IVPAG(INDEX,NODES,FCN,FCNJ,A,TIDG,TIEND,
     1                        TOL,PARAM,Y)
ICOUNT=ICOUNT+1

C Calculate MW from moments and write results
```

```
IF(T.EQ.1.0.OR.ICOUNT.EQ.PCOUNT) THEN

FIRST=Y(5)+Y(8)
FETA=Y(5)/FIRST
FLAM=Y(8)/FIRST

RMWN=RMERMW*(FETA*Y(5)/Y(4)+FLAM*Y(8)/Y(7))
RMWW=RMERMW*(FETA*Y(6)/Y(5)+FLAM*Y(9)/Y(8))
RPD=RMWW/RMWN
WTETD=Y(3)*TETDMW*(VP/(VP+VW))*(100./1.077)*(1./.4)

WRITE(13,10) T/3600.,RMWW,RMWN,RPD,Y(1)/TWO,Y(2),Y(3)/TTO
WRITE(14,10) T/3600.,Y(10),Y(11),Y(12),FS/FSO,FA/FAO,FV
WRITE(15,10) T/3600.,Y(4),Y(5),Y(6),Y(7),Y(8),Y(9)
ICOUNT=0
ENDIF
        ENDDO

C CLOSE DATA FILES

CLOSE(UNIT=13)
CLOSE(UNIT=14)
CLOSE(UNIT=15)
STOP
END


C*************************************************************************

C SUPPORTING ALGEBRAIC CALCULATIONS

SUBROUTINE ALGBR
DIMENSION DY(12)

COMMON/MISC/ ETA3,DY,PCOUNT,RMERMW,SIMTIM,TSTEP,TWO,TTO
COMMON/PART/ AP,RKM,RPC,SAP,SVP,VW
COMMON/RKS/  RK1,RK2,RK3,RK6,RK7,RKRED
COMMON/SITES/ FS,FA,FV,FSO,FAO,FVO
COMMON/STEP/ T,TETDMW,TEPMW,VP,STETD,STEPN

OPEN(UNIT=11,NAME='RCP1.DAT',TYPE='OLD')
```

```
      OPEN(UNIT=12,NAME='CNST1.DAT',TYPE='OLD')

      15 FORMAT(E10.4, 18( / E10.4))
      20 FORMAT(E10.4, 22( / E10.4))

      READ(11,15) GSUL,GTEPN,GTETD,STEPN,STETD,VW,WP,DPART,
           1              DNM,FCONV,FSULINC,RMN,RMW,FAO,FVO,TEMP,
           1              TSTEP,SIMTIM,RPCOUNT
      PCOUNT=RPCOUNT

      READ(12,20) A1,ER1,A2,ER2,A3,ER3,A6,ER6,A7,ER7,
           1              RMEDCOR1,RMEDCOR2,RMEDCOR3,RMEDCOR6,RMEDCOR7,
           1              RKRED,RKM,RPC,RMONMW,SULMW,TEPMW,TETDMW,RPI


      C CALCULATE INITIAL CONDITIONS FOR ODEs

      DY(1)=GTEPN*0.47/(TEPMW*VW) !TW
      TWO=DY(1)
      DY(2)=0.0 !TP
      VP=WP/DPART
      DY(3)=GTETD/(TETDMW*VP) !TT
      TTO=DY(3)

      GSULINC=GSUL*FSULINC
      RMERMW=RMONMW*(1.+GSULINC/(FCONV*100.))

      DY(5)=FCONV*100./(RMONMW*VP) !ETA1
      DY(4)=DY(5)/(RMN/RMERMW) !ETA0
      DY(6)=DY(5)*(RMW/RMERMW) !ETA2
      ETA3=(DY(6)/(DY(4)*DY(5)))*(2.*DY(4)*DY(6)-DY(5)**2.)

      DY(7)=0.0 !LAM0
      DY(8)=0.0 !LAM1
      DY(9)=0.0 !LAM2

      C CALCULATE INITIAL SULFUR AND CHLORINE REACTIVE SITES

      DY(10)=GSULINC/(SULMW*6.*VP) !RSO
      DY(11)=FCONV*100.*FAO/(RMONMW*VP) !ACO
      DY(12)=FCONV*100.*FVO/(RMONMW*VP) !VCO
```

```
FSO=DY(10)/DY(5)
FS=FSO
FA=FAO
FV=FVO

C CALCULATE RATE CONSTANTS

RK1=A1*EXP(-ER1/TEMP) !CC/MOL-SEC
RK2=A2*EXP(-ER2/TEMP)
RK3=A3*EXP(-ER3/TEMP)
RK6=A6*EXP(-ER6/TEMP)
RK7=A7*EXP(-ER7/TEMP)

C     Apply medium correctioon

RK1=RK1*RMEDCOR1
RK2=RK2*RMEDCOR2
RK3=RK3*RMEDCOR3*5.0
RK6=RK6*RMEDCOR6
RK7=RK7*RMEDCOR7

C CALCULATE MASS TRANSFER-RELATED VARIABLES

DCM=DNM*1.0E-07
SAP=RPI*(DCM**2.)
SVP=(RPI/6.)*(DCM**3.)
RNP=VP/SVP
AP=SAP*RNP

CLOSE(UNIT=11)
CLOSE(UNIT=12)
RETURN
END

C*************************************************************************

C ODEs

SUBROUTINE FCN(NODES,TIDG,Y,YPRIME)

DIMENSION Y(NODES),YPRIME(NODES),DY(12)
```

```
COMMON/MISC/ ETA3,DY,PCOUNT,RMERMW,SIMTIM,TSTEP,TWO,TTO
COMMON/PART/ AP,RKM,RPC,SAP,SVP,VW
COMMON/RKS/  RK1,RK2,RK3,RK6,RK7,RKRED
COMMON/SITES/ FS,FA,FV,FSO,FAO,FVO
COMMON/STEP/ T,TETDMW,TEPMW,VP,STETD,STEPN

C Adjust k1 and k2 for sulfur linkage reactivity

RK1ADJ=RK1*FS+2.*RK1*RKRED*(FSO-FS)
RK2ADJ=RK2*FS+2.*RK2*RKRED*(FSO-FS)

YPRIME(1)=-(RKM*AP/VW)*(Y(1)-(1./RPC)*Y(2))

IF(STEPN.GT.0.AND.T.EQ.86400.) THEN
YPRIME(1)=YPRIME(1)+(GTEPN*0.47/(TEPMW*VW))/TSTEP
ENDIF

YPRIME(2)=(RKM*SAP/SVP)*(Y(1)-(1./RPC)*Y(2))
     1             -RK1ADJ*Y(2)*(Y(5)-Y(4))+RK6*Y(3)*Y(7)

YPRIME(3)=-RK6*Y(3)*Y(7)

IF(STETD.GT.0.AND.T.EQ.86400.) THEN
YPRIME(3)=YPRIME(3)+(STETD/(TETDMW*VP))/TSTEP
ENDIF

ETA01=0.0
ETA02=0.0
ETA03=0.0
ETA06=RK6*Y(3)*Y(7)
ETA07=0.0
YPRIME(4)=ETA01+ETA02+ETA03+ETA06+ETA07

ETA11=-(RK1ADJ*Y(2)/2.)*(Y(6)-Y(5))
ETA12=RK2ADJ*( Y(8)*(Y(5)-Y(4))-(Y(7)/2.)*(Y(6)-Y(5)) )
ETA13=RK3*FA*Y(8)*Y(5)
ETA16=RK6*Y(3)*Y(8)
ETA17=RK7*FV*Y(8)*Y(5)
YPRIME(5)=ETA11+ETA12+ETA13+ETA16+ETA17

ETA21=(RK1ADJ*Y(2)/6.)*(Y(5)+3.*Y(6)-4.*ETA3)
ETA22=RK2ADJ*( Y(9)*(Y(5)-Y(4))+Y(8)*(Y(6)-Y(5))-
```

```
     1         (Y(7)/6.)*(4.*ETA3-3.*Y(6)-Y(5)))
ETA23=RK3*FA*(2.*Y(8)*Y(6)+Y(9)*Y(5))
ETA26=RK6*Y(3)*Y(9)
ETA27=RK7*FV*(2.*Y(8)*Y(6)+Y(9)*Y(5))
YPRIME(6)=ETA21+ETA22+ETA23+ETA26+ETA27

ETA3=( Y(6)/(Y(4)*Y(5)) )*( 2.*Y(4)*Y(6)-Y(5)**2. )

RLAM01=RK1ADJ*Y(2)*(Y(5)-Y(4))
RLAM02=0.0
RLAM03=-RK3*FA*Y(5)*Y(7)
RLAM06=-RK6*Y(3)*Y(7)
RLAM07=-RK7*FV*Y(5)*Y(7)
YPRIME(7)=RLAM01+RLAM02+RLAM03+RLAM06+RLAM07

RLAM11=(RK1ADJ*Y(2)/2.)*(Y(6)-Y(5))
RLAM12=-RK2ADJ*(Y(8)*(Y(5)-Y(4))-(Y(7)/2.)*(Y(6)-Y(5)))
RLAM13=-RK3*FA*Y(5)*Y(8)
RLAM16=-RK6*Y(3)*Y(8)
RLAM17=-RK7*FV*Y(5)*Y(8)
YPRIME(8)=RLAM11+RLAM12+RLAM13+RLAM16+RLAM17

RLAM21=(RK1ADJ*Y(2)/6.)*(Y(5)-3.*Y(6)+2.*ETA3)
RLAM22=-RK2ADJ*(Y(9)*(Y(5)-Y(4))-
     1          (Y(7)/6.)*(2.*ETA3-3.*Y(6)+Y(5)))
RLAM23=-RK3*FA*Y(5)*Y(9)
RLAM26=-RK6*Y(3)*Y(9)
RLAM27=-RK7*FV*Y(5)*Y(9)
YPRIME(9)=RLAM21+RLAM22+RLAM23+RLAM26+RLAM27

YPRIME(10)=-RK1*FS*Y(2)*(Y(5)-Y(4))
YPRIME(11)=-RK3*FA*Y(5)*Y(7)
YPRIME(12)=-RK7*FV*Y(5)*Y(7)

FS=Y(10)/(Y(5)+Y(8))
FA=Y(11)/(Y(5)+Y(8))
FV=Y(12)/(Y(5)+Y(8))

RETURN
END

SUBROUTINE FCNJ(NODES,TIDG,Y,PD)
```

```
      DIMENSION Y(NODES),PD(NODES,NODES)
      RETURN
      END
```

C. Sample Input/Output File

CNST1.DAT

```
2.7500E+11 A1 frequency factor for k1 cc/mol sec
4.8660E+03 ER1 E/R for k1 K
4.6200E+11 A2 frequency factor for k2 cc/mol sec
4.5940E+03 ER2 E/R for k2 K
7.2200E+09 A3 frequency factor for k3 cc/mol sec
5.1690E+03 ER3 E/R for k3 K
3.7500E+11 A6 frequency factor for k6 cc/mol sec
4.6030E+03 ER6 E/R for k6 K
3.8800E+09 A7 frequency factor for k7 cc/mol sec
8.4980E+03 ER7 E/R for k7 K
4.0000E-02 RMEDCOR1 medium corr for k1
3.0000E-03 RMEDCOR2 medium corr for k2
3.1500E-02 RMEDCOR3 medium corr for k3
2.5000E-03 RMEDCOR6 medium corr for k6
3.1500E-02 RMEDCOR7 medium corr for k7
1.0000E-02 RKRED reactive site access corr
6.4000E-10 RKM  mass transfer coeff cm/sec
6.6667E-03 RPC Tepidone partition coeff
8.8540E+01 RMONMW monomer MW g/mole
3.2060E+01 SULMW sulfur MW g/mole
2.2739E+02 TEPMW Tepidone MW g/mole
2.9656E+02 TETDMW TETD MW g/mole
3.1416E+00 pi
```

RCP1.DAT

```
0.6000E+00 GSUL   grams S phm
0.7990E+00 GTEPN  grams Tepidone N phm
0.4348E+00 GTETD  grams TETD phm
0.0000E+00 STEPN  grams step Tepidone N phm
0.0000E+00 STETD  grams step TETD phm
1.1533E+02 VW aqueos volume cc phm
1.0663E+02 WP particle phase g phm
1.1603E+00 DPART particle phase g/cc
1.0000E+02 DNM wgt-avg particle diam nm
0.8400E+00 FCONV frac conv at begin pep
0.5000E+00 FSULINC frac recipe S incor in polymer
1.0500E+05 RMN MWn of unpeptized polymer g/mole
1.5790E+06 RMW MWw of unpeptized polymer g/mole
0.0100E+00 FAO init frac allylic Cl
0.9900E+00 FVO init frac vinyl Cl
3.1315E+02 TEMP temperature K
1.0000E+01 TSTEP ODE solution freq sec
2.0000E+01 SIMTIM simulation time hrs
3.6000E+01 PCOUNT data write count
```

MOLWGT.DAT (labels not present)

t, hrs	MWw	MWn	PD	Tw/Two	Tp	TT/TTo
.0000E+00	.1579E+07	.1050E+06	.1504E+02	.1000E+01	.0000E+00	.1000E+01
.1000E+00	.1192E+07	.1421E+06	.8391E+01	.9701E+00	.7290E-07	.9836E+00
.2000E+00	.1037E+07	.1262E+06	.8217E+01	.9480E+00	.7169E-07	.9624E+00
.3000E+00	.9306E+06	.1156E+06	.8054E+01	.9266E+00	.7035E-07	.9426E+00
.4000E+00	.8527E+06	.1080E+06	.7897E+01	.9062E+00	.6911E-07	.9240E+00
.5000E+00	.7938E+06	.1023E+06	.7759E+01	.8865E+00	.6797E-07	.9066E+00
.6000E+00	.7480E+06	.9785E+05	.7645E+01	.8677E+00	.6690E-07	.8903E+00
.7000E+00	.7118E+06	.9424E+05	.7553E+01	.8497E+00	.6590E-07	.8751E+00
continued . . .						

SITES.DAT (labels not present)

t, hrs	[RS]	[AC]	[VC]	fs/fso	fa/fao	fv
.0000E+00	.1697E-04	.1032E-03	.1022E-01	.1000E+01	.1000E+01	.9900E+00
.1000E+00	.1624E-04	.1029E-03	.1022E-01	.9570E+00	.9970E+00	.9900E+00
.2000E+00	.1551E-04	.1025E-03	.1022E-01	.9137E+00	.9931E+00	.9900E+00
.3000E+00	.1481E-04	.1021E-03	.1022E-01	.8726E+00	.9893E+00	.9900E+00
.4000E+00	.1414E-04	.1017E-03	.1022E-01	.8335E+00	.9857E+00	.9900E+00
.5000E+00	.1352E-04	.1014E-03	.1022E-01	.7965E+00	.9822E+00	.9900E+00
.6000E+00	.1292E-04	.1010E-03	.1022E-01	.7613E+00	.9788E+00	.9900E+00
.7000E+00	.1236E-04	.1007E-03	.1022E-01	.7282E+00	.9757E+00	.9900E+00
continued . . .						

MOMENT.DAT (labels not present)

t, hrs	eta0	eta1	eta2	lambda0	lambda1	lambda2
.0000E+00	.8736E-05	.1032E-01	.1834E+03	.0000E+00	.0000E+00	.0000E+00
.1000E+00	.8998E-05	.9280E-02	.1208E+03	.1568E-06	.1043E-02	.1778E+02
.2000E+00	.9335E-05	.9437E-02	.1074E+03	.1530E-06	.8854E-03	.1306E+02
.3000E+00	.9652E-05	.9563E-02	.9809E+02	.1461E-06	.7595E-03	.1002E+02
.4000E+00	.9948E-05	.9658E-02	.9105E+02	.1394E-06	.6645E-03	.8010E+01
.5000E+00	.1023E-04	.9732E-02	.8560E+02	.1329E-06	.5903E-03	.6609E+01
.6000E+00	.1048E-04	.9792E-02	.8131E+02	.1268E-06	.5308E-03	.5590E+01
.7000E+00	.1073E-04	.9841E-02	.7787E+02	.1209E-06	.4819E-03	.4822E+01
continued . . .						

APPENDIX IV

Indexing Terms

G-TYPE NEOPRENE
AGING
PEPTIZATION
MATHEMATICAL MODEL